

Supporting Information

A Facile Strategy for π -Extended BOPYINs: Transformation into Six-Membered BODIPY Analogues and Their Optical Properties

Ziyi Zhang^[a], Xi Li^[a], Yilin Feng^[a], Xin Gao,^[a] Yong Qi, ^[a] Jiaying Yan,^[ab] Nuonuo Zhang,^[ab]

^aCollege of Materials and Chemical Engineering, Key Laboratory of Inorganic Nonmetallic Crystalline and Energy Conversion Materials, China Three Gorges University, Yichang, Hubei 443002, P. R. China

^bHubei Three Gorges Laboratory, Yichang, Hubei 443007, P. R. China

*Corresponding Email: nnzhang2015@ctgu.edu.cn and yanjiaying327@126.com

Content

1. Materials and methods	2
2. Quantum yield method.....	2
3. Calculation	2
4. General procedure	3
5. NMR and HRMS	8
6. UV-Vis and fluorescence data and spectra	27
7. Single Crystal.....	34

1. Materials and methods

All reagents and solvents were obtained from commercial sources and used without further purification, unless otherwise noted. All chromatographic separations were carried out on silica gel (300-400 mesh). ^1H NMR and ^{13}C NMR spectra were recorded on Bruker 400 MHz spectrometer at 298 K. DMSO- d_6 was used as solvent and TMS as internal reference. The chemical shifts were reported in parts per million (δ) relative to the appropriate reference signal: DMSO- d_6 (the quintet centered at 2.50 ppm). High resolution mass spectra were measured on Bruker APCI or SYNAPT G2 analysis instrument. UV-Vis spectra in various solvents were detected on Shimadzu UV-2600 spectrometer in 10 mm quartz cell. Fluorescence spectra were obtained using a Shimadzu FL-4500 spectrometer, emission wavelengths λ are reported in nm.

2. Quantum yield method

Relative fluorescence quantum efficiencies of compounds **7** ~ **8** and **10** ~ **11** were obtained by comparing the areas under the corrected emission spectrum of the test sample in various solvents with Fluorescein ($\Phi_f=0.9$ in 0.1 M NaOH) for **7** ~ **8** and **10** ~ **11**. Non-degassed, spectroscopic grade solvents and a 10 mm quartz cuvette were used. Dilute solutions ($0.01 < A < 0.05$) were used to minimize the reabsorption effects. Quantum yields were determined using the following equation:

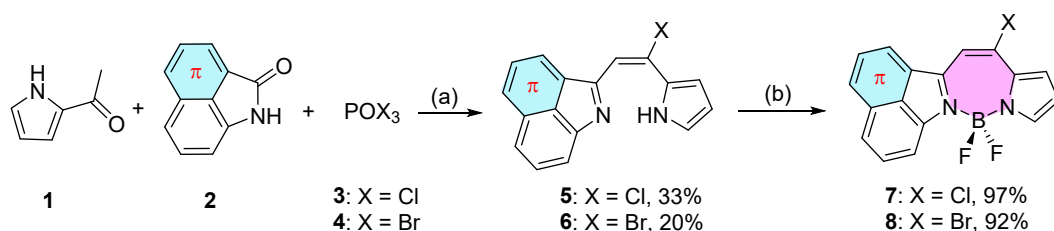
$$\Phi_X = \Phi_S (I_X/I_S) (A_S/A_X) (n_X/n_S)^2$$

Where Φ_S stands for the reported quantum yield of the standard, I stands for the integrated emission spectra, A stands for the absorbance at the excitation wavelength and stands for the refractive index of the solvent being used. X subscript stands for the test sample, and S subscript stands for the standard.

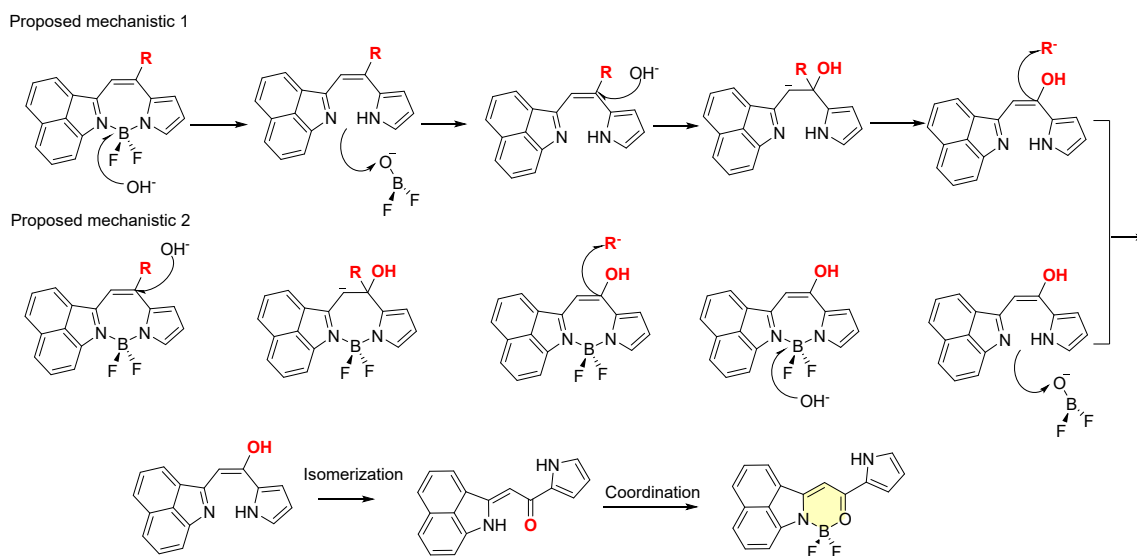
3. Calculation

All calculations were performed with the Gaussian software package¹, employing the Integral Equation Formalism Polarizable Continuum Model (IEFPCM) solvation model. Geometry optimizations were performed at the B3LYP/6-311G(d, p) level. Transition state and excited state were performed at the B3LYP/6-31G(d) level. Vibrational frequencies were done with harmonic approximation to make sure that all the geometric structures had no imaginary frequency and the transition state geometries had only one imaginary frequency. The single point energy on the energy profiles are further calculated at B3LYP/6-311G(d, p) calculation level due to its higher accuracy. TD-DFT calculation were performed at the CAM-B3LYP/6-31G(d) level.

4. General procedure



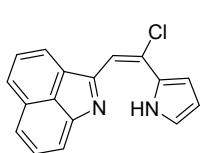
Scheme S1 Synthesis method of π -extended BOPYIN skeleton. (a): Toluene (Tol), reflux, 3h, (b):Et₃N, BF₃·Et₂O, Tol, reflux, 10min.



Scheme S2 The proposed mechanistic schemes for the conversion of BOPYIN derivatives to the six-membered BODIPY analogue **11**

4.1 General procedure of **5** ~ **9** and **11** ~ **12**

5

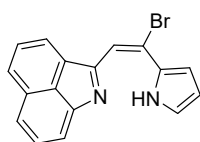


A mixture of 1,8-naphthalimide (507.55 mg, 3.0 mmol) and 2-acetylpyrrole (491.10 mg, 4.5 mmol) was dissolved in toluene (25 mL). The reaction mixture was heated to 120 °C in an oil bath, followed by the slow dropwise addition of POCl₃ (825 μ L, 9.0 mmol).

The system was refluxed for 3 h, and the reaction progress was monitored by thin-layer chromatography (TLC). After completion, the mixture was quenched with water and neutralized to pH 8 using an aqueous NaOH solution. The organic phase was extracted with dichloromethane, concentrated under reduced pressure, and dried. Purification by column chromatography (petroleum ether/dichloromethane, v/v) afforded **5** as a dark

red solid with a green metallic luster in 33% yield. ^1H NMR (400 MHz, Chloroform- d) δ 15.93 (s, 1H), 8.06 – 8.00 (m, 2H), 7.83 – 7.76 (m, 2H), 7.71 (d, J = 7.5 Hz, 1H), 7.62 (dd, J = 8.4, 6.9 Hz, 1H), 7.29 – 7.26 (m, 1H), 7.04 – 6.98 (m, 2H), 6.46 – 6.42 (m, 1H). ^{13}C NMR (101 MHz, Chloroform- d) δ 162.51, 151.21, 136.91, 136.86, 130.73, 130.00, 129.70, 129.32, 128.54, 127.76, 125.91, 124.83, 123.81, 121.08, 117.63, 111.28, 109.83. HRMS(ESI) Calcd for $\text{C}_{17}\text{H}_{12}\text{ClN}_2[\text{M}+\text{H}]^+$: 279.0689, found 279.0770.

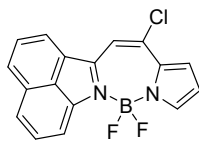
6



The reaction was carried out following the same procedure as described for compound **5**, but with POCl_3 replaced by POBr_3 , affording compound **6** in 15% yield. ^1H NMR (400 MHz, Chloroform- d) δ 15.94 (s, 1H), 8.01 (dd, J = 7.5, 4.1 Hz, 2H), 7.83

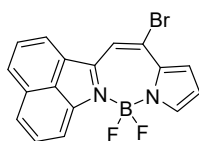
– 7.76 (m, 2H), 7.69 (t, J = 7.5 Hz, 1H), 7.65 – 7.58 (m, 1H), 7.30 (d, J = 2.0 Hz, 1H), 7.25 (s, 1H), 7.05 – 7.00 (m, 1H), 6.46 – 6.40 (m, 1H). ^{13}C NMR (101 MHz, Chloroform- d) δ 162.69, 151.09, 136.74, 131.00, 130.72, 129.70, 129.29, 128.53, 127.78, 127.67, 126.01, 124.91, 124.01, 121.23, 120.28, 113.55, 111.43. HRMS(ESI) Calcd for $\text{C}_{17}\text{H}_{12}\text{BrN}_2[\text{M}+\text{H}]^+$: 323.0184, found 323.0191.

7



Intermediate **5** (278.06 mg, 1.0 mmol) was dissolved in toluene (10 mL) and heated to 120 °C. Subsequently, triethylamine (Et_3N , 417 μL , 3.0 mmol) and boron trifluoride diethyl etherate ($\text{BF}_3 \cdot \text{Et}_2\text{O}$) were added sequentially. The reaction mixture was refluxed for 10 min, and the completion of the reaction was monitored by thin-layer chromatography (TLC). After removal of the solvent under reduced pressure, the crude product was purified by column chromatography using a mixture of petroleum ether and ethyl acetate (25:1, v/v) as the eluent, affording **7** as a black solid with a green metallic luster in 97% yield. ^1H NMR (400 MHz, $\text{DMSO}-d_6$) δ 8.71 (d, J = 7.2 Hz, 1H), 8.35 (d, J = 7.9 Hz, 1H), 8.07 (d, J = 7.4 Hz, 1H), 7.97 (d, J = 8.2 Hz, 1H), 7.88 (t, J = 7.6 Hz, 1H), 7.76–7.68 (m, 2H), 7.52 (s, 1H), 7.31 (d, J = 3.9 Hz, 1H), 6.65 (dd, J = 4.0, 2.2 Hz, 1H). ^{13}C NMR (101 MHz, $\text{DMSO}-d_6$) δ 143.3, 142.2, 135.4, 133.7, 132.6, 131.3, 130.6, 130.4, 130.1, 129.0, 127.4, 124.2, 123.6, 120.9, 120.8, 114.6, 105.7. HRMS(ESI) Calcd for $\text{C}_{17}\text{H}_{10}\text{BClF}_2\text{N}_2\text{Na}[\text{M}+\text{Na}]^+$: 349.0491, found 349.0497.

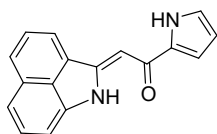
8



The target compound was synthesized using an analogous procedure to that of **7**, with **6** being employed as the starting material instead of **5**. The target compound **8** was obtained as a black solid exhibiting green metallic luster, with a yield of 92%. ^1H NMR (400 MHz, $\text{DMSO}-d_6$) δ 8.86 (d, J = 7.3 Hz, 1H), 8.48 (d, J = 8.0 Hz, 1H), 8.17 (d, J = 7.3 Hz, 1H), 8.10 (d, J = 8.2 Hz, 1H), 7.97 (t, J = 7.6 Hz, 1H), 7.83–7.74 (m, 3H), 7.29 (d, J = 3.9 Hz, 1H), 6.63 (dd, J = 3.9, 2.2 Hz, 1H). ^{13}C NMR (101 MHz, $\text{DMSO}-d_6$) δ 157.5, 142.2,

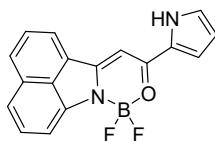
135.4, 135.2, 134.0, 133.7, 131.1, 130.7, 130.4, 130.2, 129.0, 127.5, 125.9, 124.2, 121.0, 114.7, 109.2. HRMS(ESI) Calcd for $C_{17}H_{10}BBrF_2N_2Na[M+Na]^+$: 392.9986, found 392.9993.

9



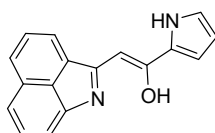
Under the standard conditions, a solution of parent dye **7** (326 mg, 1.0 mmol) in a mixed solvent of dichloromethane (10 mL) and methanol (10 mL) was treated dropwise with an aqueous NaOH solution (60 mg, 1.5 mmol in 1 mL H_2O) at 40 °C. The resulting mixture was stirred at the same temperature for 8 h, during which TLC monitoring indicated complete consumption of the starting material and full conversion to product **9**. After concentration under reduced pressure, the crude product was purified by column chromatography (petroleum ether/dichloromethane, v/v = 5:2) to afford **9** as a yellow solid in 79% yield. 1H NMR (400 MHz, $DMSO-d_6$) δ 11.64 (s, 1H), 11.31 (s, 1H), 8.20 (d, J = 7.1 Hz, 1H), 7.97 (d, J = 8.0 Hz, 1H), 7.72 (t, J = 7.6 Hz, 1H), 7.48 – 7.39 (m, 2H), 7.11 (d, J = 5.9 Hz, 2H), 7.05 (d, J = 3.1 Hz, 1H), 6.96 (s, 1H), 6.23 (dd, J = 3.8, 2.1 Hz, 1H). ^{13}C NMR (101 MHz, $DMSO-d_6$) δ 179.54, 151.78, 142.89, 134.25, 133.28, 130.44, 129.99, 129.14, 128.70, 125.88, 124.40, 121.40, 118.24, 114.06, 110.02, 106.30, 92.28. HRMS (ESI) Calcd. for $C_{17}H_{13}N_2O [M+H]^+$: 261.1032, found 261.1028.

11



A solution of either **9** or **12** (261.1 mg, 1.0 mmol) in anhydrous toluene (25 mL) was charged sequentially with triethylamine (697 μ L, 5 mmol) and boron trifluoride diethyl etherate (634 μ L, 5 mmol) under nitrogen atmosphere. The reaction mixture was heated to reflux (120°C) with vigorous stirring for 20 minutes, with reaction progress monitored by thin-layer chromatography (TLC). Upon complete consumption of starting material as confirmed by TLC analysis, the mixture was concentrated under reduced pressure. The crude product was purified by flash column chromatography using a petroleum ether/dichloromethane (3:1, v/v) gradient system to afford **11** as an orange-red crystalline solid in 98% isolated yield. 1H NMR (600 MHz, $DMSO-d_6$) δ 12.43, 8.49 (d, J = 6.9 Hz), 8.35 (d, J = 7.8 Hz), 7.94 (t, J = 7.3 Hz), 7.85 (d, J = 8.1 Hz), 7.68 (t, J = 7.4 Hz), 7.54 (d, J = 6.9 Hz), 7.43, 7.39, 7.34, 6.43. ^{13}C NMR (151 MHz, $DMSO-d_6$) δ 166.26, 160.68, 142.03, 133.48, 130.37, 130.17, 130.02, 128.78, 127.64 (d, J = 11.7 Hz), 126.09, 123.70, 118.45, 113.75, 112.83, 89.09. HRMS (ESI) Calcd. for $C_{17}H_{11}N_2ONaBF_2 [M+Na]^+$: 331.0828, found 331.0830.

12



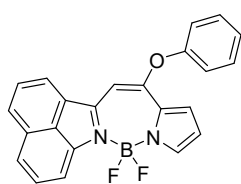
5 (278 mg, 1.0 mmol) was dissolved in a mixed solvent of dichloromethane (10 mL) and methanol (10 mL), to which an aqueous solution of sodium hydroxide (60 mg, 1.5 mmol in 1 mL

H₂O) was added dropwise. The reaction mixture was stirred at room temperature for 4 h, with the reaction progress monitored by thin-layer chromatography (TLC). Upon completion of the reaction as indicated by TLC, the mixture was concentrated under reduced pressure. The crude product was purified by column chromatography using a mixture of petroleum ether and dichloromethane (v/v = 5:1) as eluent to afford **12** as a rose-red solid in 70% yield. ¹H NMR (400 MHz, DMSO-d₆) δ 11.65 (s, 1H), 11.31 (s, 1H), 8.20 (d, J = 7.1 Hz, 1H), 7.97 (d, J = 8.0 Hz, 1H), 7.72 (t, J = 7.6 Hz, 1H), 7.47 – 7.40 (m, 2H), 7.11 (d, J = 6.2 Hz, 2H), 7.05 (s, 1H), 6.97 (s, 1H), 6.25 – 6.20 (m, 1H). ¹³C NMR (101 MHz, DMSO-d₆) δ 179.52, 151.76, 142.90, 134.24, 133.28, 130.43, 130.00, 129.15, 128.70, 125.87, 124.41, 121.41, 118.23, 114.07, 110.02, 106.31, 92.29. HRMS (ESI) Calcd. for C₁₇H₁₃N₂O [M+H]⁺: 261.1025, found 261.1028.

4.2 General procedure of **10a** ~ **10e**

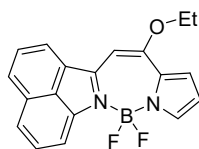
A solution of the parent dye **7** (326 mg, 1.0 mmol) in dichloromethane (10 mL) was treated sequentially with reagents **a**~**e** (10.0 mmol each) and cesium carbonate (1.3 g, 4.0 mmol). The reaction mixture was heated to 60 °C and refluxed for 1.5~8 h, with progress monitored by TLC until completion. After quenching with water, the organic phase was extracted with dichloromethane, concentrated under reduced pressure, and dried. Purification by column chromatography using a mixed eluent of petroleum ether/dichloromethane (v/v) afforded the target compounds **10a**~**e** as dark red solids in yields ranging from 52% to 95%.

10a



Following the general procedure, product **10a** was obtained as a dark red solid in 93% yield. ¹H NMR (400 MHz, DMSO-d₆) δ 8.43 (d, J = 8.0 Hz, 1H), 8.22 (d, J = 7.3 Hz, 1H), 8.09 (d, J = 7.3 Hz, 1H), 8.01 (d, J = 8.2 Hz, 1H), 7.89 (t, J = 7.7 Hz, 1H), 7.79 (t, J = 7.8 Hz, 1H), 7.70 (s, 1H), 7.57 (t, J = 8.0 Hz, 2H), 7.33 (td, J = 15.1, 13.9, 5.6 Hz, 4H), 6.64-6.56 (m, 2H). ¹³C NMR (101 MHz, DMSO-d₆) δ 162.9, 154.7, 134.4, 130.5, 130.3, 129.9, 129.2, 128.1, 125.7, 125.6, 120.1, 118.9, 113.4, 92.3. HRMS (ESI) Calcd for C₂₃H₁₅BF₂N₂ONa [M+Na]⁺: 407.1143, found 407.1148.

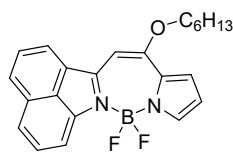
10b



Following the general procedure, product **10b** was obtained as a dark red solid in 65% yield. ¹H NMR (400 MHz, DMSO-d₆) δ 8.78 (d, J = 7.2 Hz, 1H), 8.37 (d, J = 8.0 Hz, 1H), 7.95 (dd, J = 21.5, 7.6 Hz, 3H), 7.72 (t, J = 7.8 Hz, 1H), 7.54 (s, 1H), 7.15 (d, J = 3.7 Hz, 1H), 6.85 (s, 1H), 6.53-6.44 (m, 1H), 4.56 (q, J = 6.9 Hz, 2H), 1.51 (t, J = 6.9 Hz, 3H). ¹³C NMR (101 MHz, DMSO-d₆) δ 165.0, 143.2, 133.6, 130.3, 130.0, 129.5, 129.2, 128.2, 124.8,

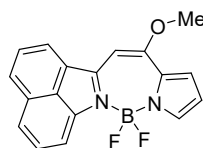
118.6, 112.1, 87.3, 66.1, 14.3. HRMS(ESI) Calcd for $C_{19}H_{15}BF_2N_2ONa[M+Na]^+$: 359.1143, found 359.1149.

10c



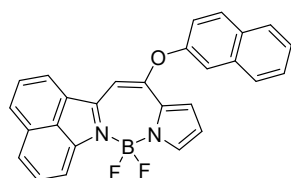
Following the general procedure, product **10c** was obtained as a dark red solid in 85% yield. 1H NMR (400 MHz, DMSO- d_6) δ 8.74 (d, J = 7.3 Hz, 1H), 8.33 (d, J = 7.9 Hz, 1H), 7.96 (d, J = 7.2 Hz, 1H), 7.89 (dd, J = 8.1, 3.9 Hz, 2H), 7.70 (t, J = 7.6 Hz, 1H), 7.54 (s, 1H), 7.13 (d, J = 3.7 Hz, 1H), 6.83 (s, 1H), 6.49 (t, J = 3.0 Hz, 1H), 4.46 (t, J = 6.3 Hz, 2H), 1.86 (t, J = 7.2 Hz, 2H), 1.51 (t, J = 7.5 Hz, 2H), 1.35 (tt, J = 7.7, 4.6 Hz, 4H), 0.89 (t, J = 6.7 Hz, 3H). ^{13}C NMR (101 MHz, DMSO- d_6) δ 165.1, 133.6, 130.3, 130.0, 129.5, 128.2, 124.8, 118.4, 112.2, 87.3, 70.1, 30.8, 28.3, 25.2, 22.1, 13.9. HRMS(ESI) Calcd for $C_{23}H_{23}BF_2N_2ONa[M+Na]^+$: 415.1769, found 415.1776.

10d



Following the general procedure, product **10d** was obtained as a dark red solid in 52% yield. 1H NMR (400 MHz, DMSO- d_6) δ 8.82 (d, J = 7.2 Hz, 1H), 8.41 (d, J = 8.0 Hz, 1H), 7.98 (dd, J = 18.5, 7.6 Hz, 3H), 7.74 (t, J = 7.8 Hz, 1H), 7.55 (s, 1H), 7.19-7.11 (m, 1H), 6.88 (s, 1H), 6.49 (t, J = 3.0 Hz, 1H), 4.25 (s, 3H). ^{13}C NMR (101 MHz, DMSO- d_6) δ 165.6, 143.1, 133.8, 132.6, 130.3, 130.1, 129.6, 129.2, 128.3, 124.9, 124.8, 118.5, 117.9, 112.3, 86.9, 57.7. HRMS(ESI) Calcd for $C_{18}H_{13}BF_2N_2ONa[M+Na]^+$: 345.0987, found 345.0995.

10e



Following the general procedure, product **10e** was obtained as a dark red solid in 95% yield. 1H NMR (400 MHz, DMSO- d_6) δ 8.33 (d, J = 8.0 Hz, 1H), 8.16-8.08 (m, 2H), 8.09-8.00 (m, 2H), 7.95 (t, J = 7.8 Hz, 2H), 7.85 (d, J = 2.4 Hz, 1H), 7.79-7.70 (m, 3H), 7.62-7.47 (m, 3H), 7.35 (d, J = 3.8 Hz, 1H), 6.68-6.57 (m, 2H). ^{13}C NMR (101 MHz, DMSO- d_6) δ 162.9, 152.2, 142.8, 134.2, 133.9, 132.3, 131.7, 130.8, 130.6, 130.2, 129.7, 129.0, 128.2, 127.9, 127.6, 127.1, 125.8, 125.7, 124.5, 120.3, 119.9, 116.6, 113.5, 92.5. HRMS(ESI) Calcd for $C_{27}H_{17}BF_2N_2ONa[M+Na]^+$: 457.1300, found 457.1307.

5. NMR and HRMS

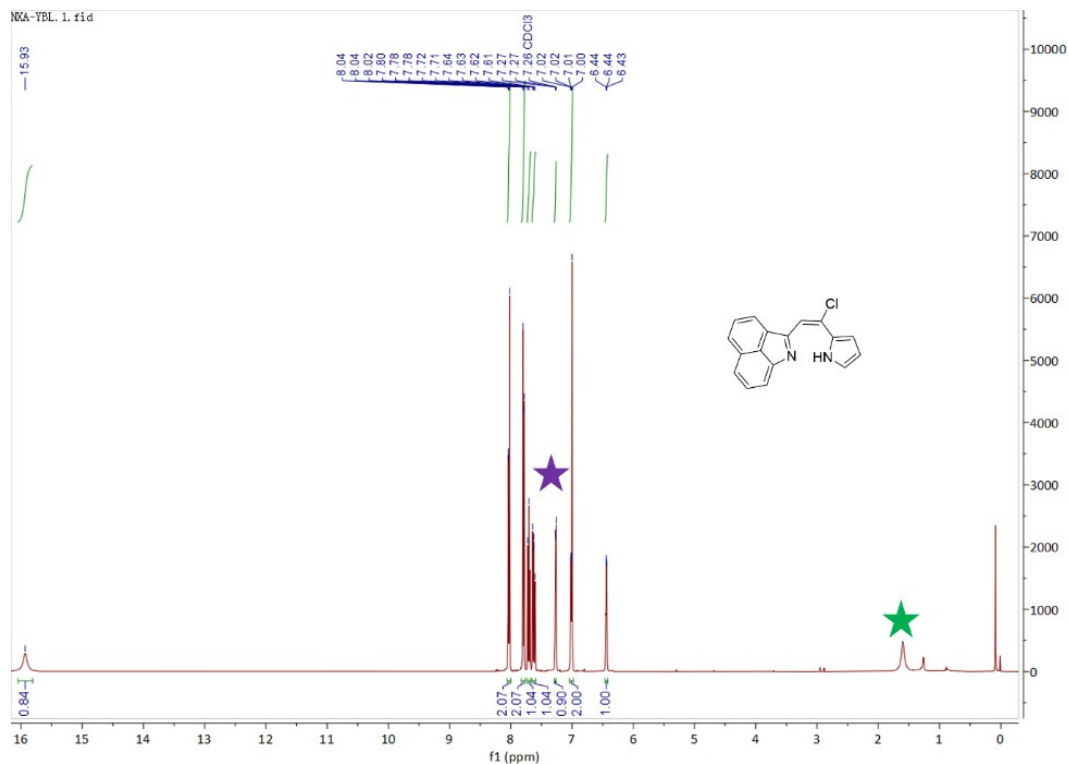


Figure S1 ^1H NMR spectra of **5** in Chloroform- d_6 (green star denotes the residual peak of H_2O , purple star denotes the solvent residual peak of Chloroform at 7.26 ppm as the referenced signal).

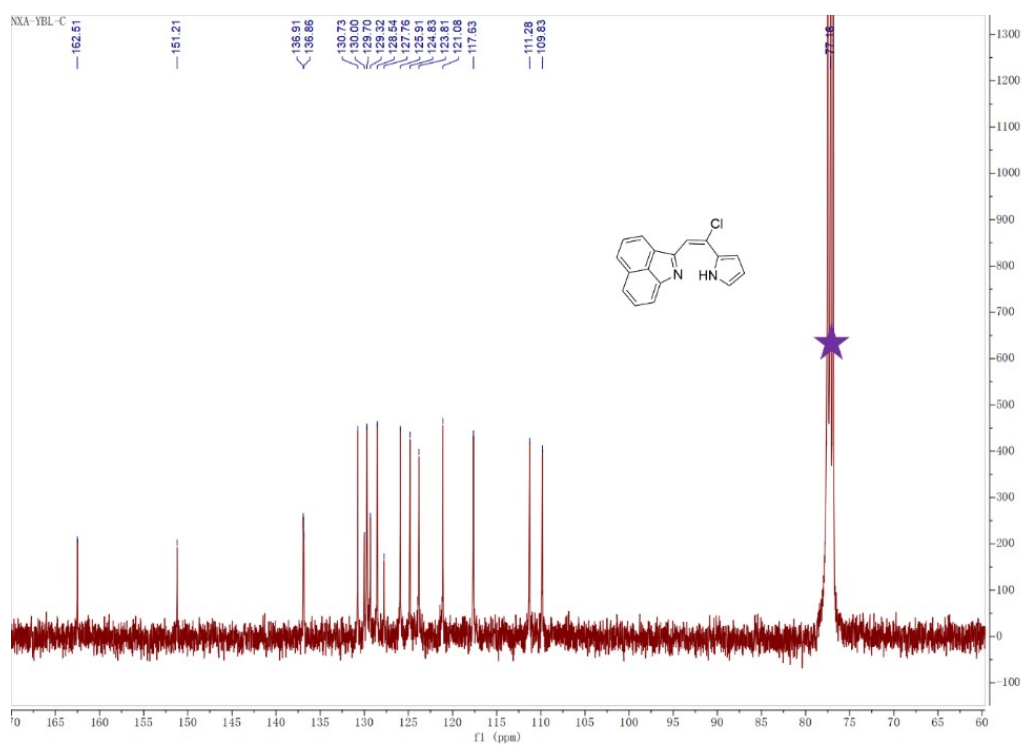


Figure S2 ^{13}C NMR spectra of **5** in Chloroform- d_6 (purple star denotes the solvent residual peak of Chloroform at 77.42 ppm as the referenced signal).

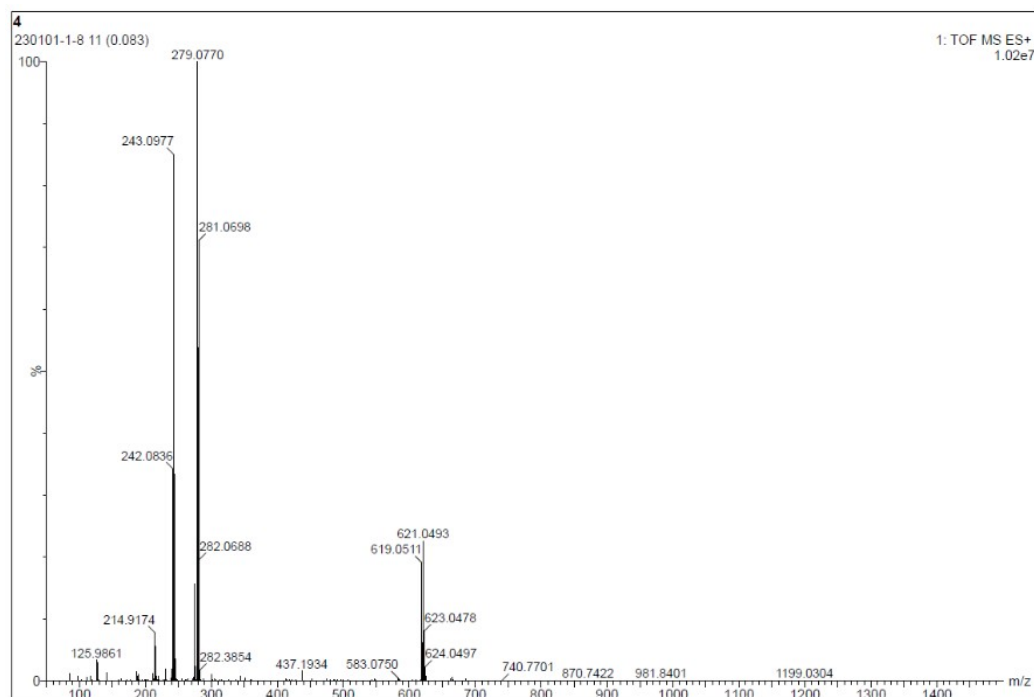


Figure S3 HR-MS spectra of **5**

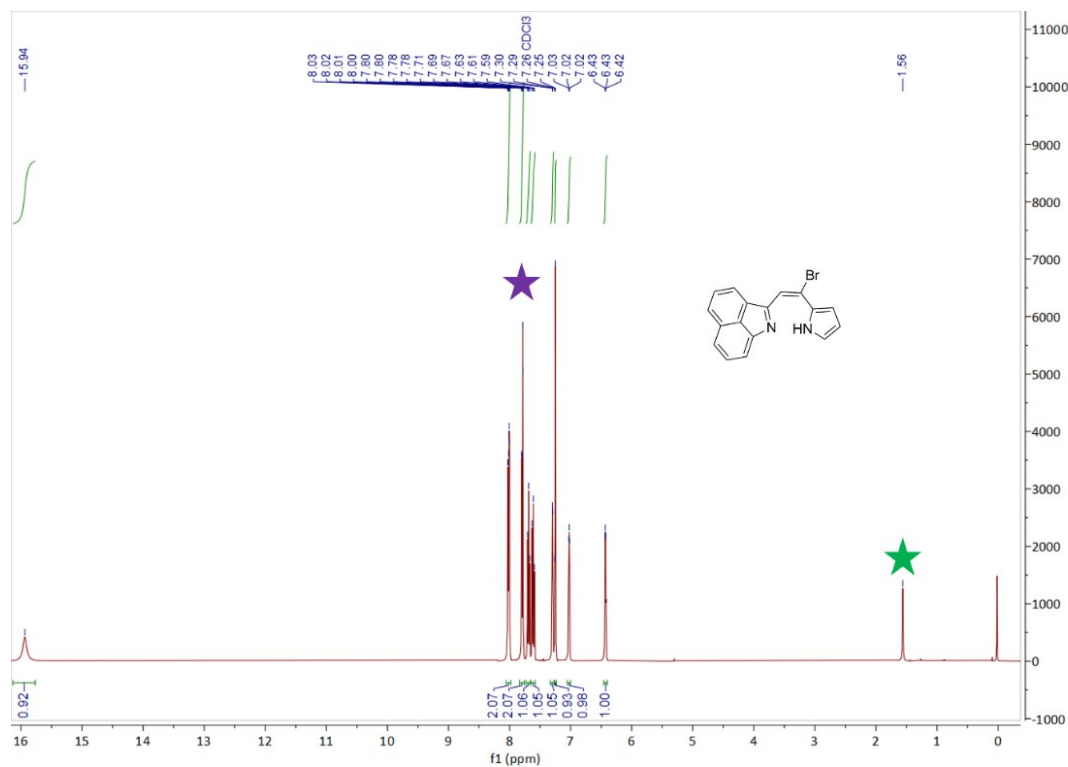


Figure S4 ^1H NMR spectra of **6** in Chloroform- d_6 (green star denotes the residual peak of H_2O , purple star denotes the solvent residual peak of Chloroform at 7.26 ppm as the referenced signal).

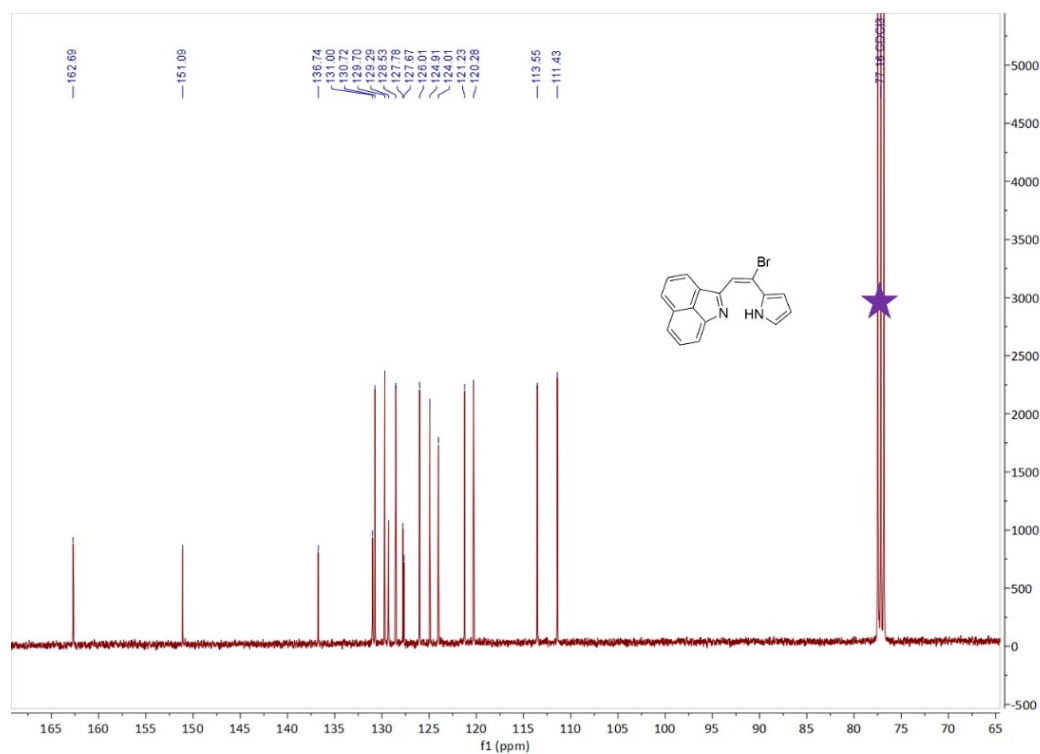


Figure S5 ¹³C NMR spectra of **6** in Chloroform-*d*₆ (purple star denotes the solvent residual peak of Chloroform at 76.57 ppm as the referenced signal).

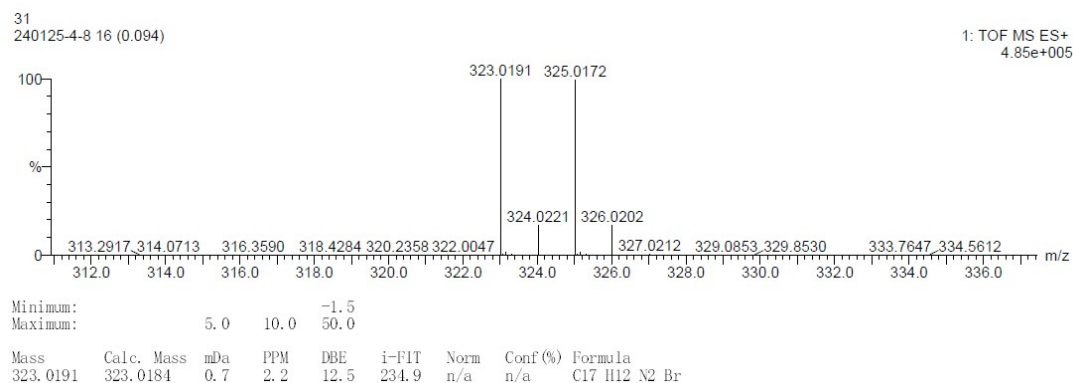


Figure S6 HR-MS spectra of **6**

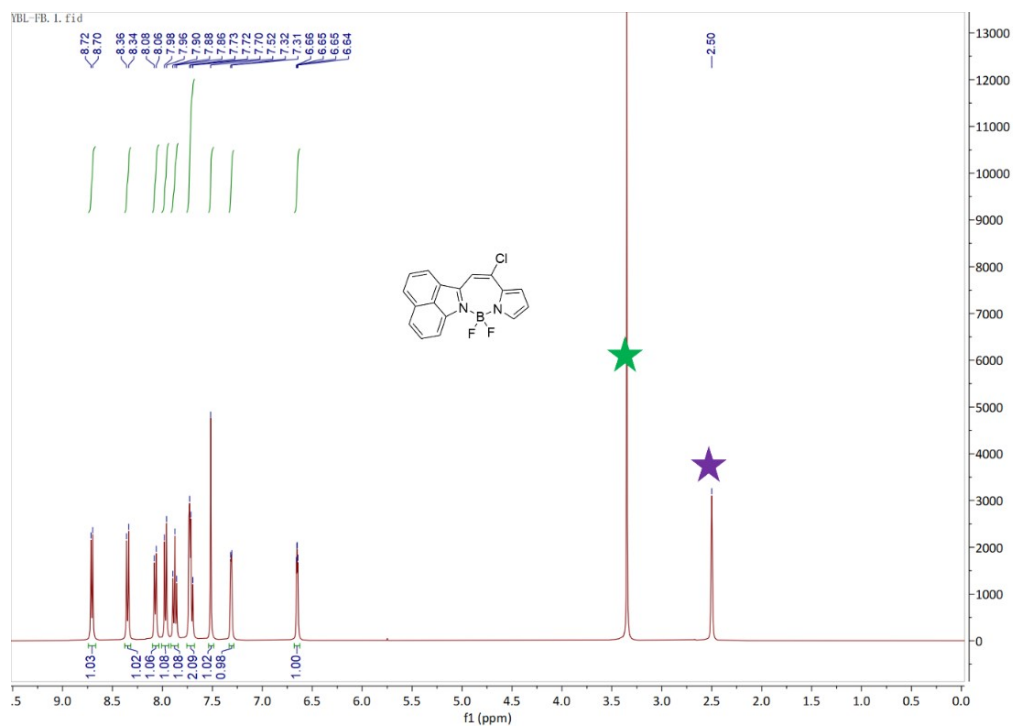


Figure S7 ^1H NMR spectra of **7** in $\text{DMSO-}d_6$ (green star denotes the residual peak of H_2O , purple star denotes the solvent residual peak of DMSO at 2.50 ppm as the referenced signal).

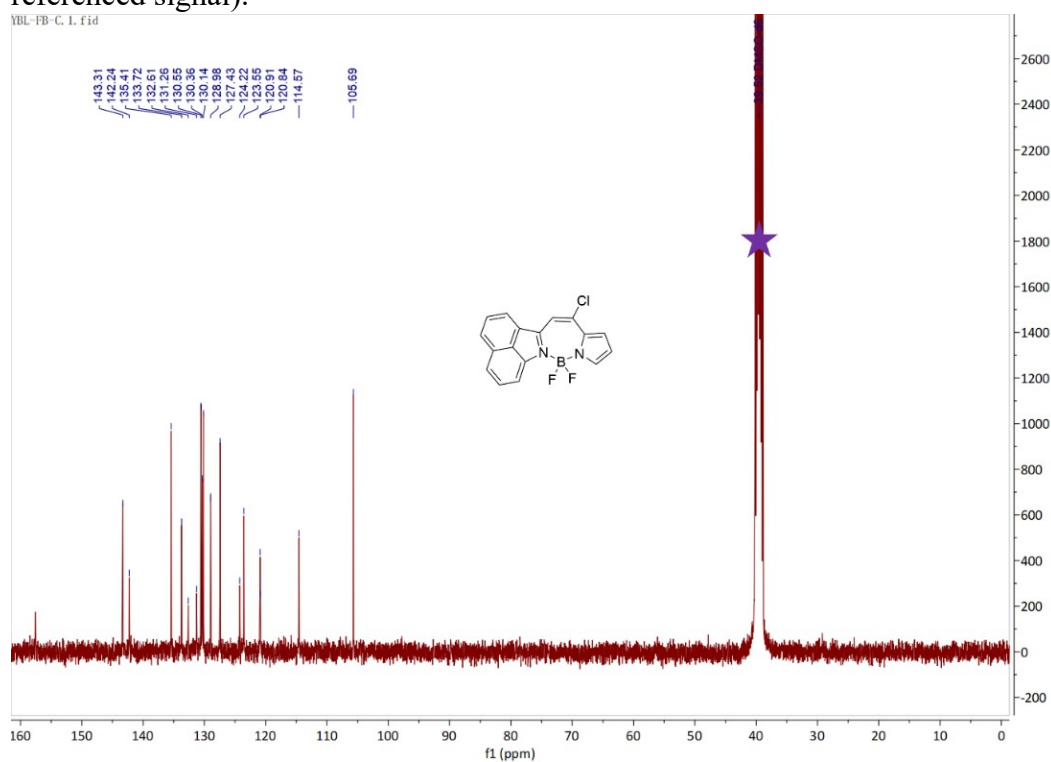


Figure S8 ^{13}C NMR spectra of **7** in $\text{DMSO-}d_6$ (purple star denotes the solvent residual peak of DMSO at 39.52 ppm as the referenced signal).

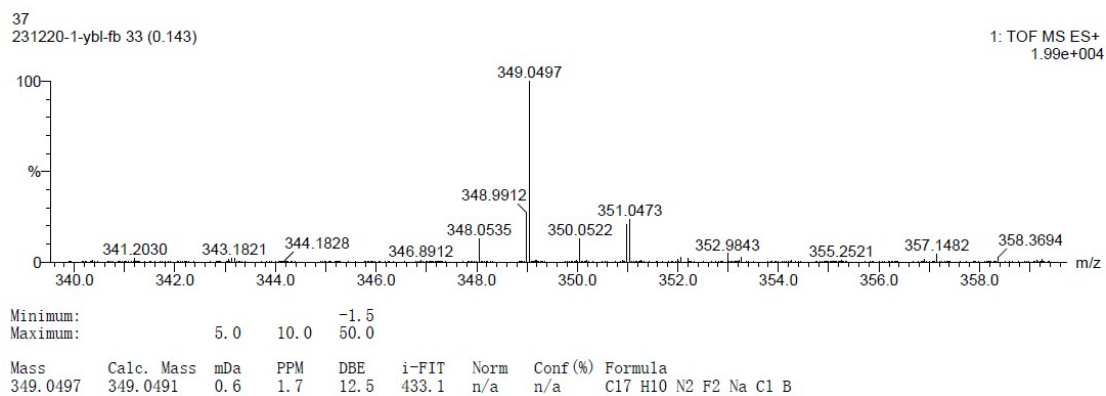


Figure S9 HR-MS spectra of **7**

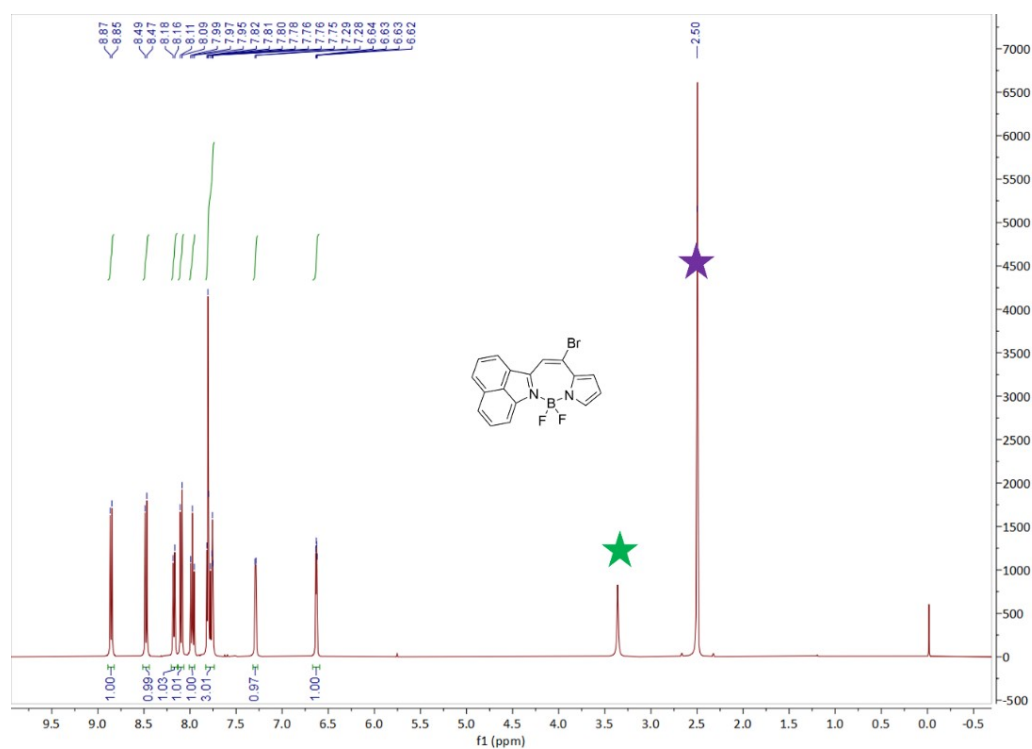


Figure S10 ^1H NMR spectra of **8** in $\text{DMSO-}d_6$ (green star denotes the residual peak of H_2O , purple star denotes the solvent residual peak of DMSO at 2.50 ppm as the referenced signal).

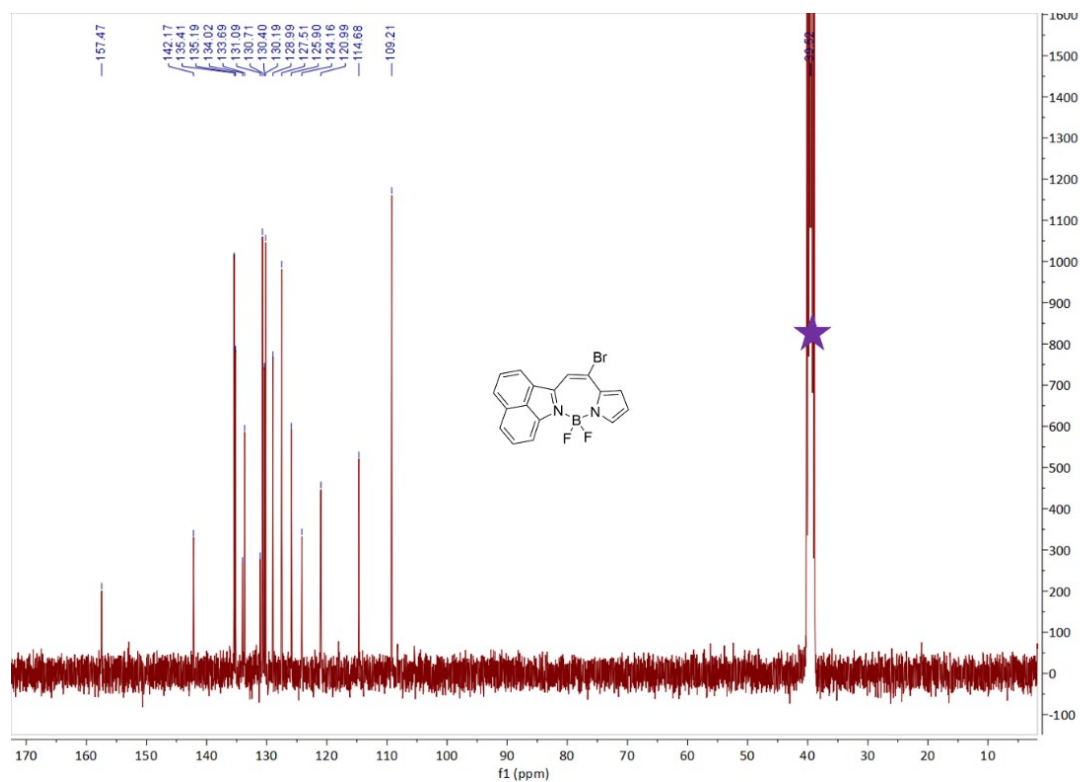


Figure S11 ¹³C NMR spectra of **8** in DMSO-*d*₆ (purple star denotes the solvent residual peak of DMSO at 39.52 ppm as the referenced signal).

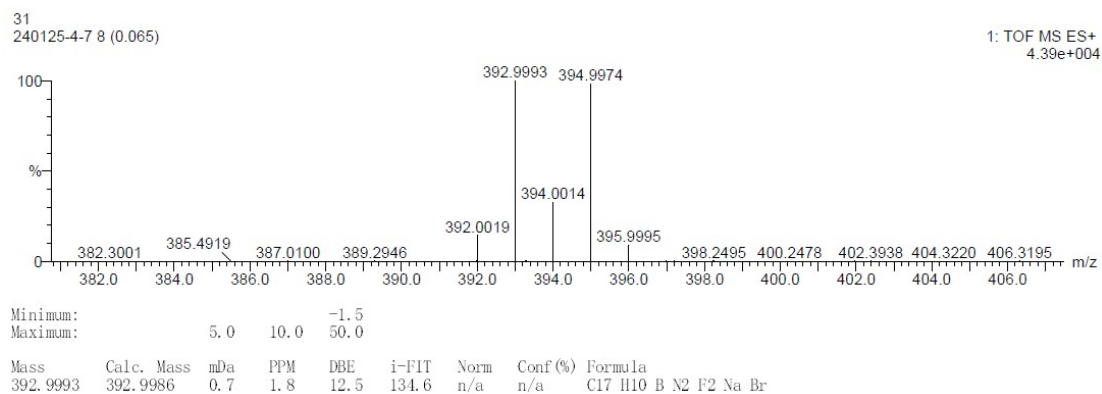


Figure S12 HR-MS spectra of **8**

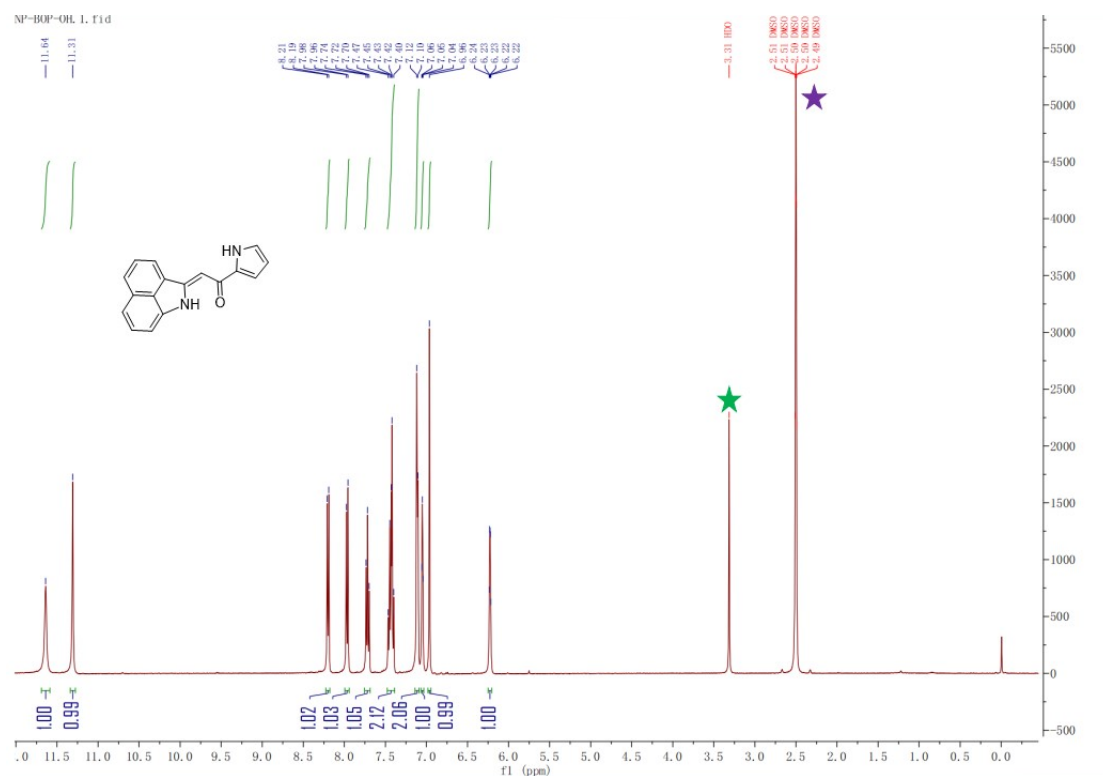


Figure S13 ¹H NMR spectra of **9** in DMSO-*d*₆ (green star denotes the residual peak of H₂O, purple star denotes the solvent residual peak of DMSO at 2.50 ppm as the referenced signal).

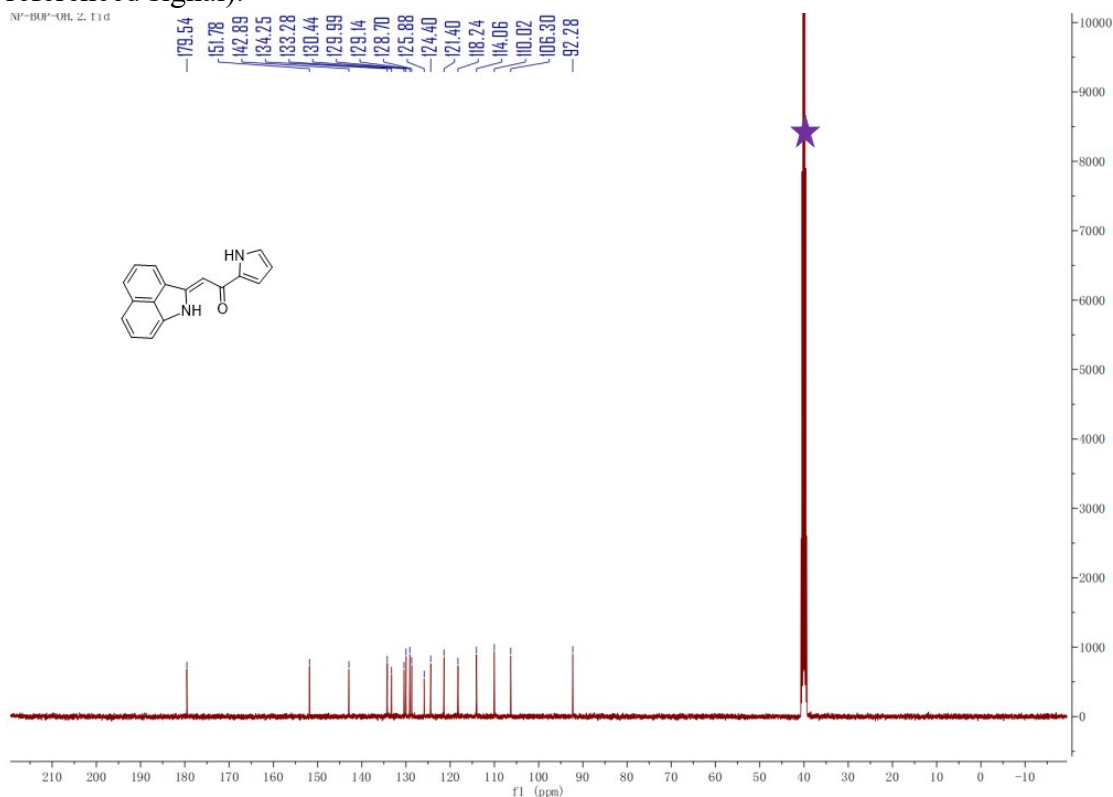


Figure S14 ¹³C NMR spectra of **9** in DMSO-*d*₆ (purple star denotes the solvent residual peak of DMSO at 39.52 ppm as the referenced signal).

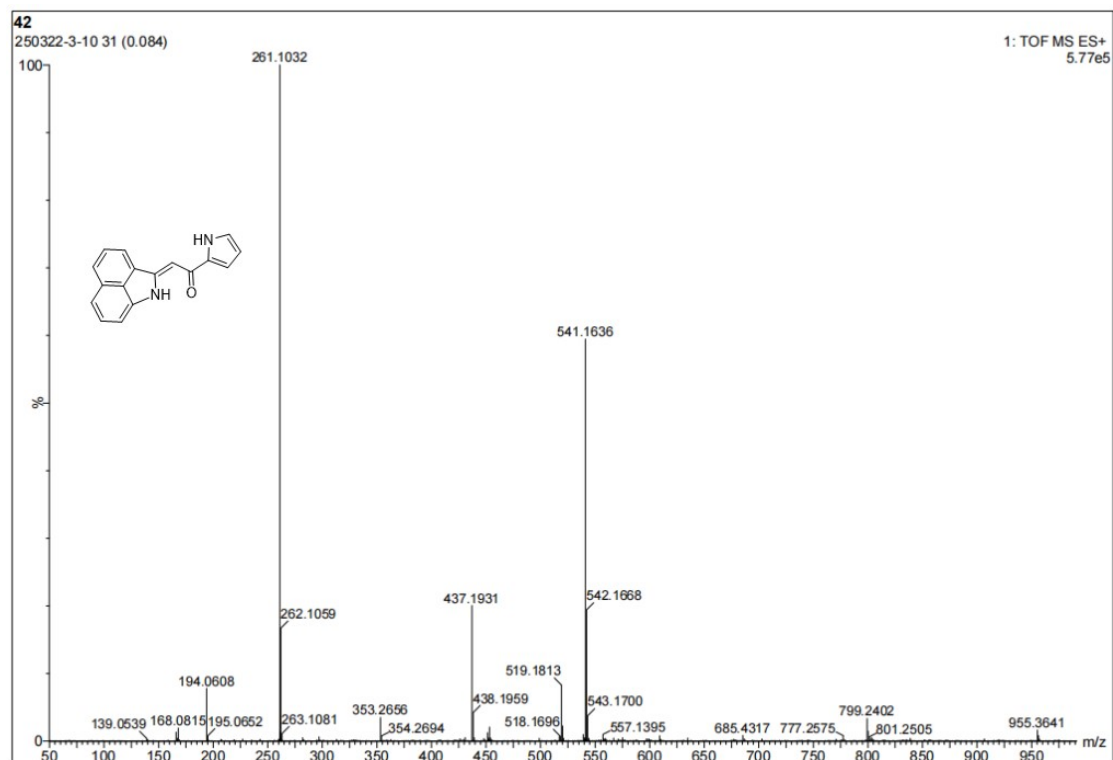


Figure S15 HR-MS spectra of **9**

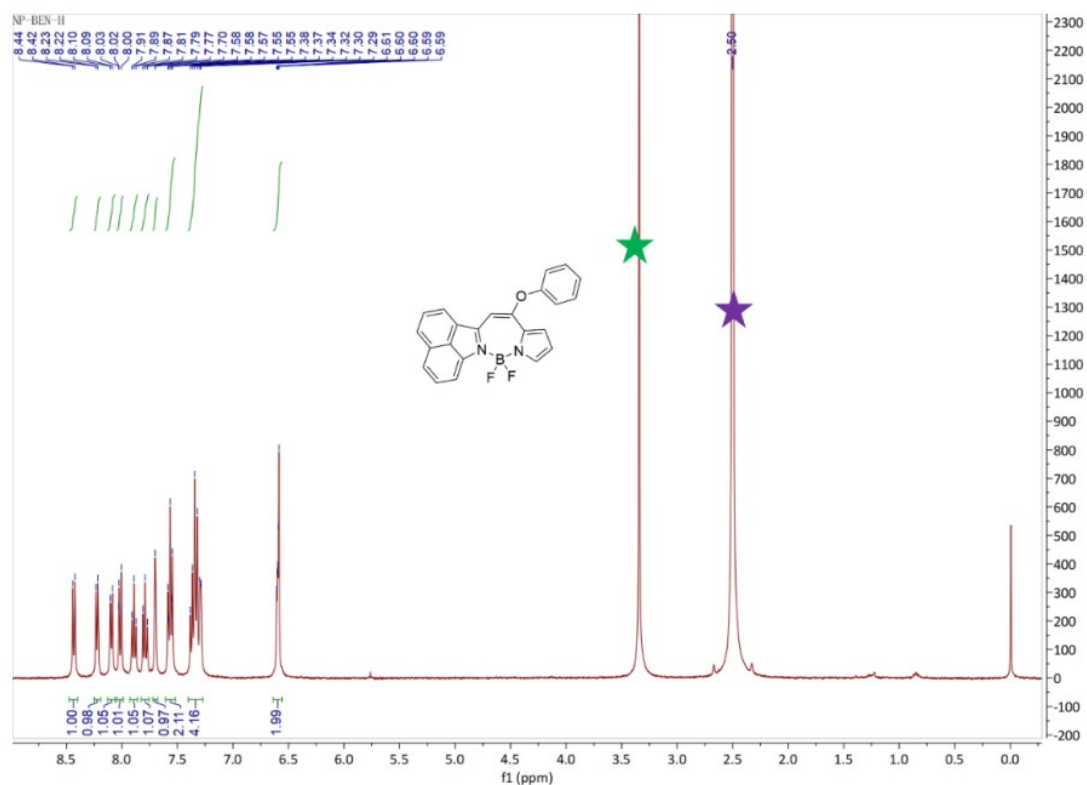


Figure S16 ^1H NMR spectra of **10a** in $\text{DMSO}-d_6$ (green star denotes the residual peak of H_2O , purple star denotes the solvent residual peak of DMSO at 2.50 ppm as the referenced signal).

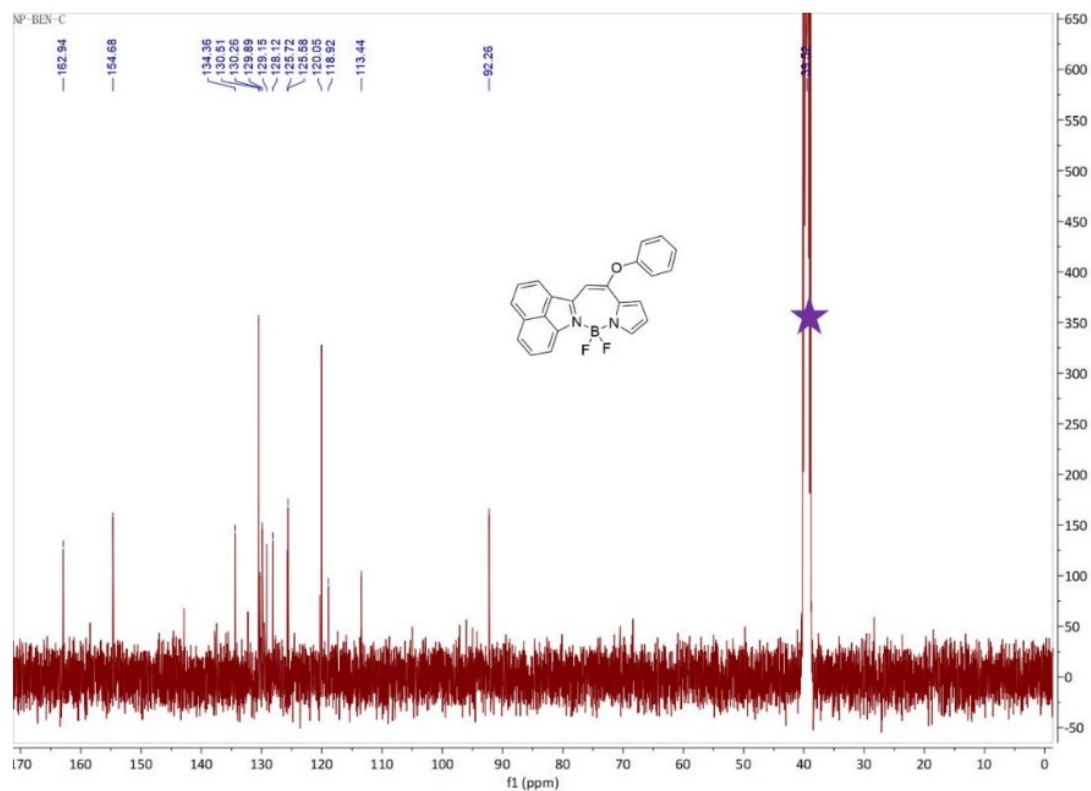


Figure S17 ¹³C NMR spectra of **10a** in DMSO-*d*₆ (purple star denotes the solvent residual peak of DMSO at 39.52 ppm as the referenced signal).

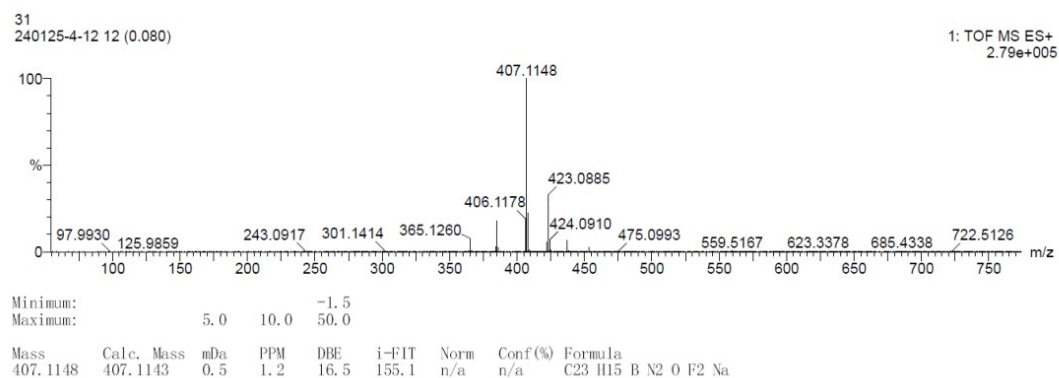


Figure S18 HR-MS spectra of **10a**

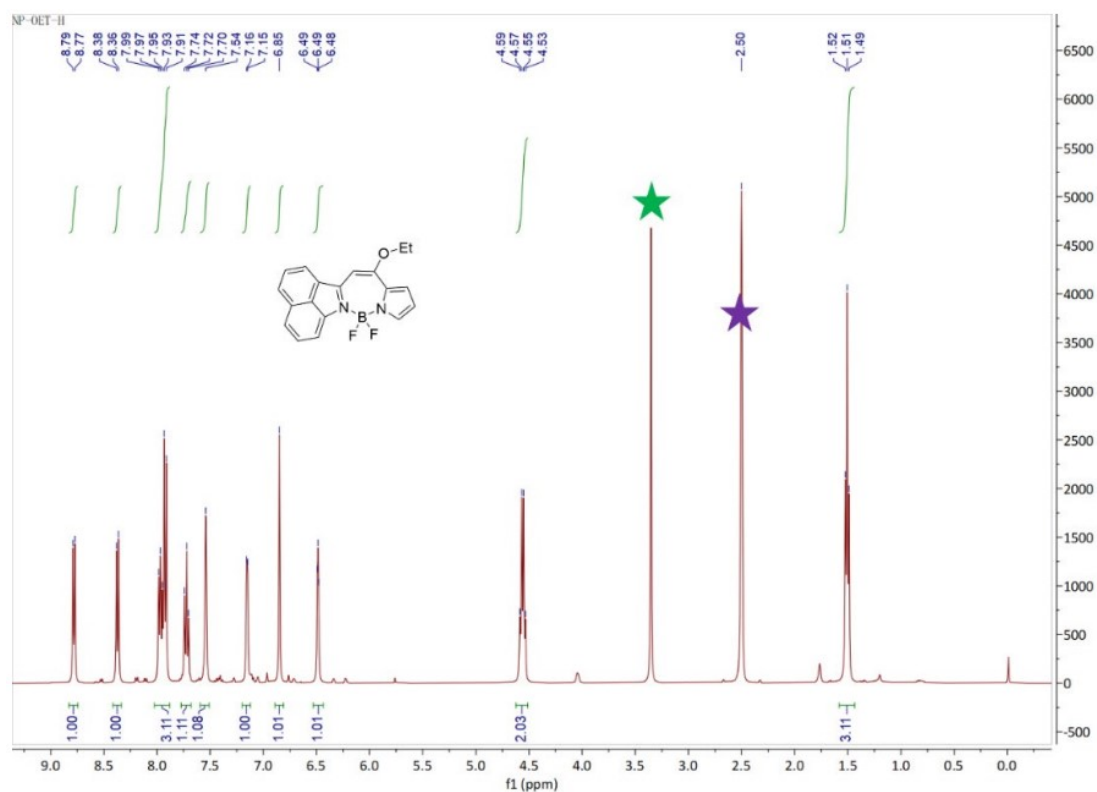


Figure S19 ^1H NMR spectra of **10b** in $\text{DMSO}-d_6$ (green star denotes the residual peak of H_2O , purple star denotes the solvent residual peak of DMSO at 2.50 ppm as the referenced signal).

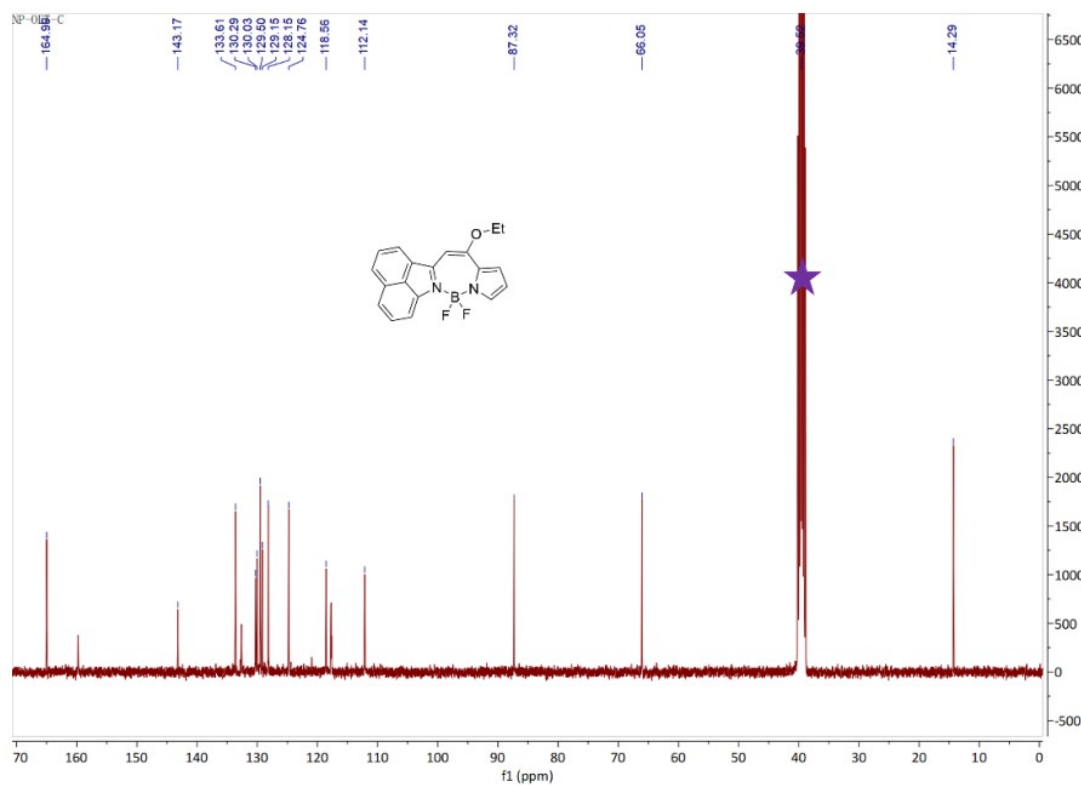


Figure S20 ^{13}C NMR spectra of **10b** in $\text{DMSO}-d_6$ (purple star denotes the solvent residual peak of DMSO at 39.52 ppm as the referenced signal).

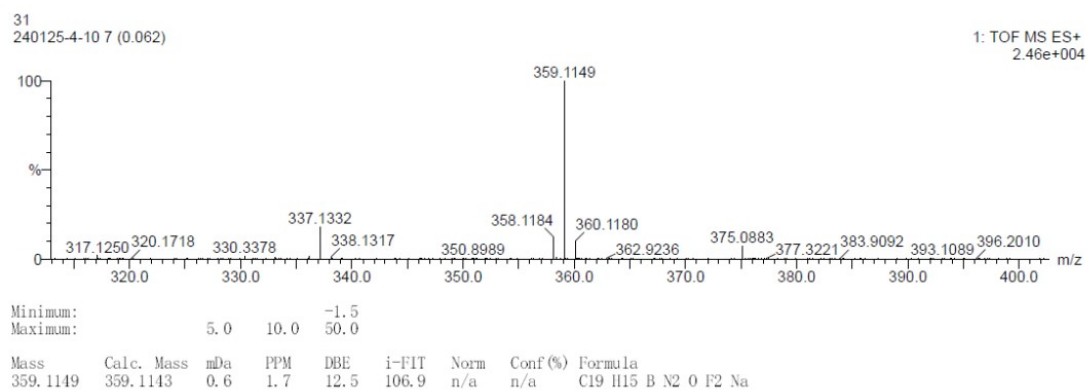


Figure S21 HR-MS spectra of **10b**

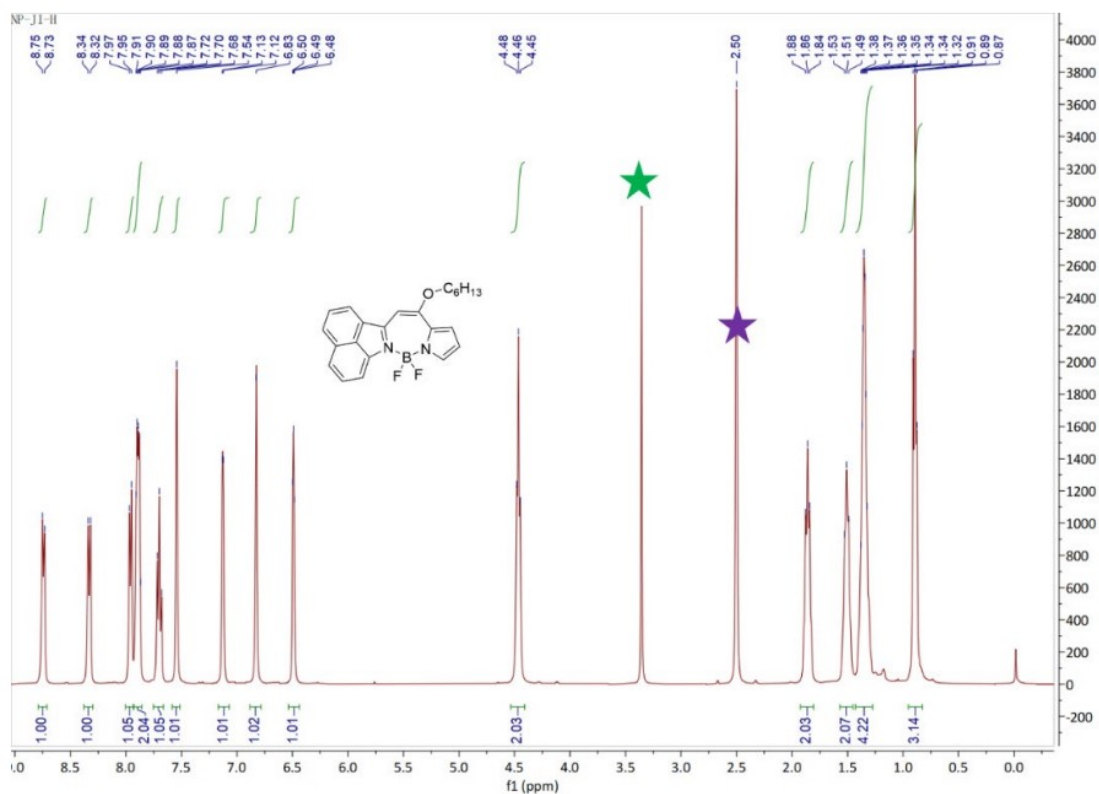


Figure S22 ^1H NMR spectra of **10c** in $\text{DMSO-}d_6$ (green star denotes the residual peak of H_2O , purple star denotes the solvent residual peak of DMSO at 2.50 ppm as the referenced signal).

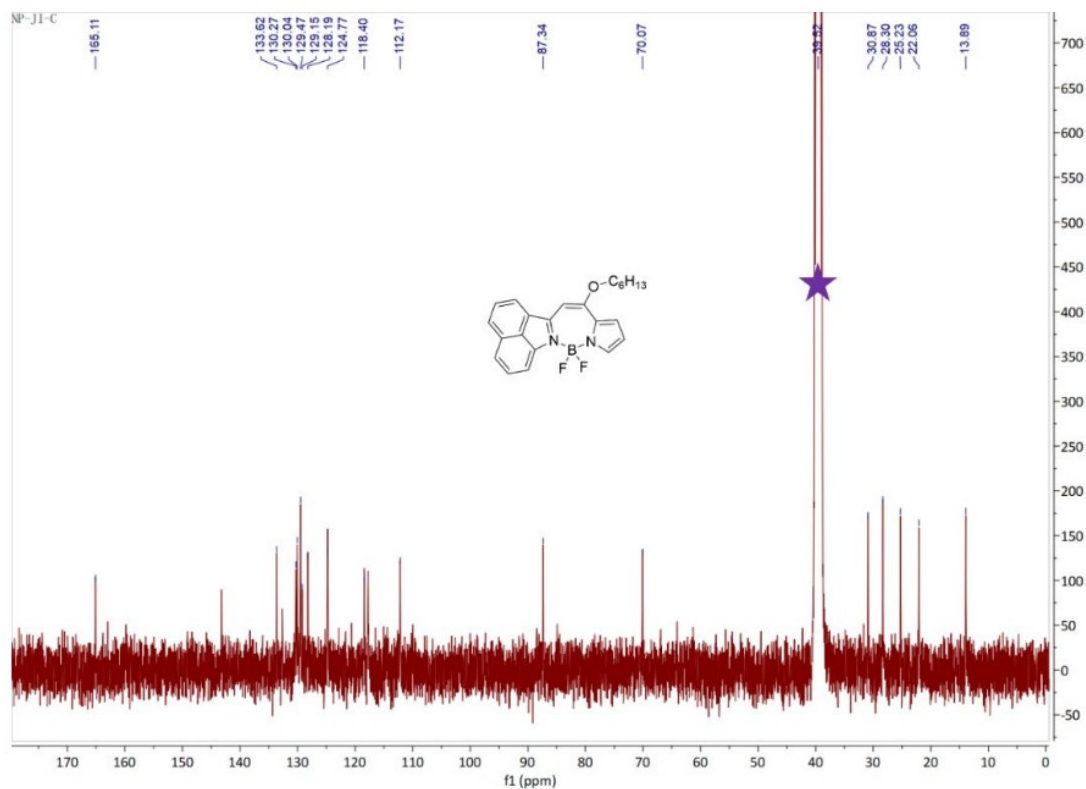


Figure S23 ^{13}C NMR spectra of **10c** in $\text{DMSO-}d_6$ (purple star denotes the solvent residual peak of DMSO at 39.52 ppm as the referenced signal).

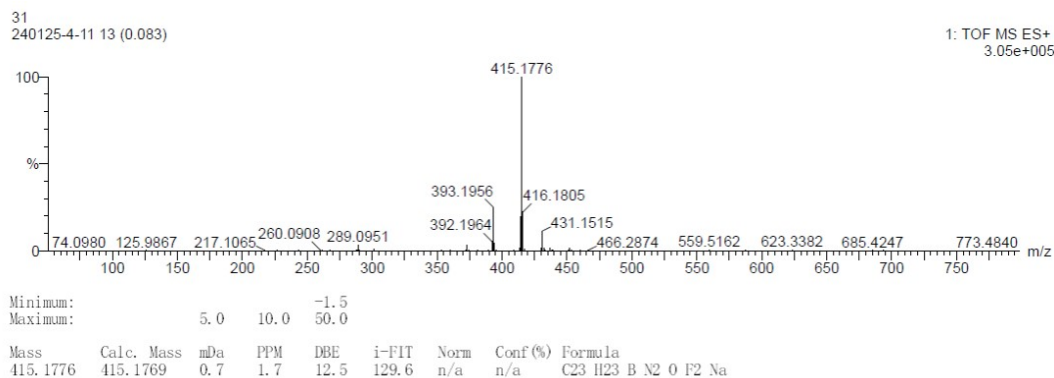


Figure S24 HR-MS spectra of **10c**

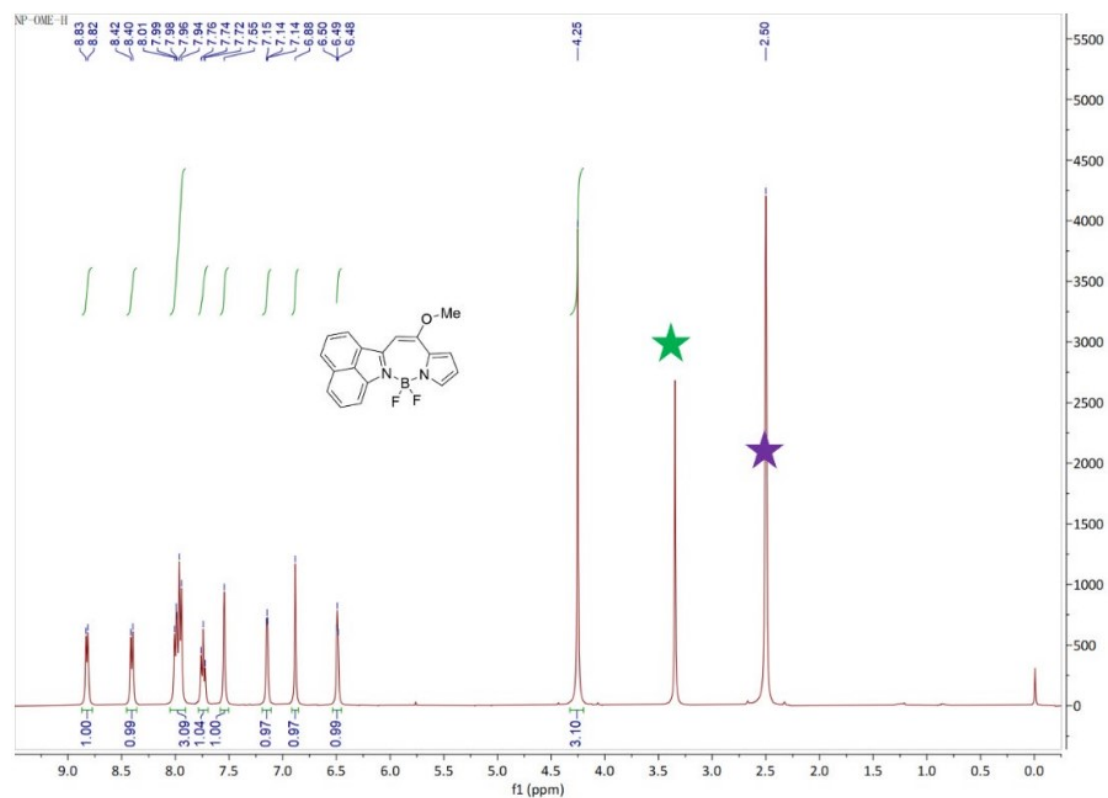


Figure S25 ^1H NMR spectra of **10d** in $\text{DMSO}-d_6$ (green star denotes the residual peak of H_2O , purple star denotes the solvent residual peak of DMSO at 2.50 ppm as the referenced signal).

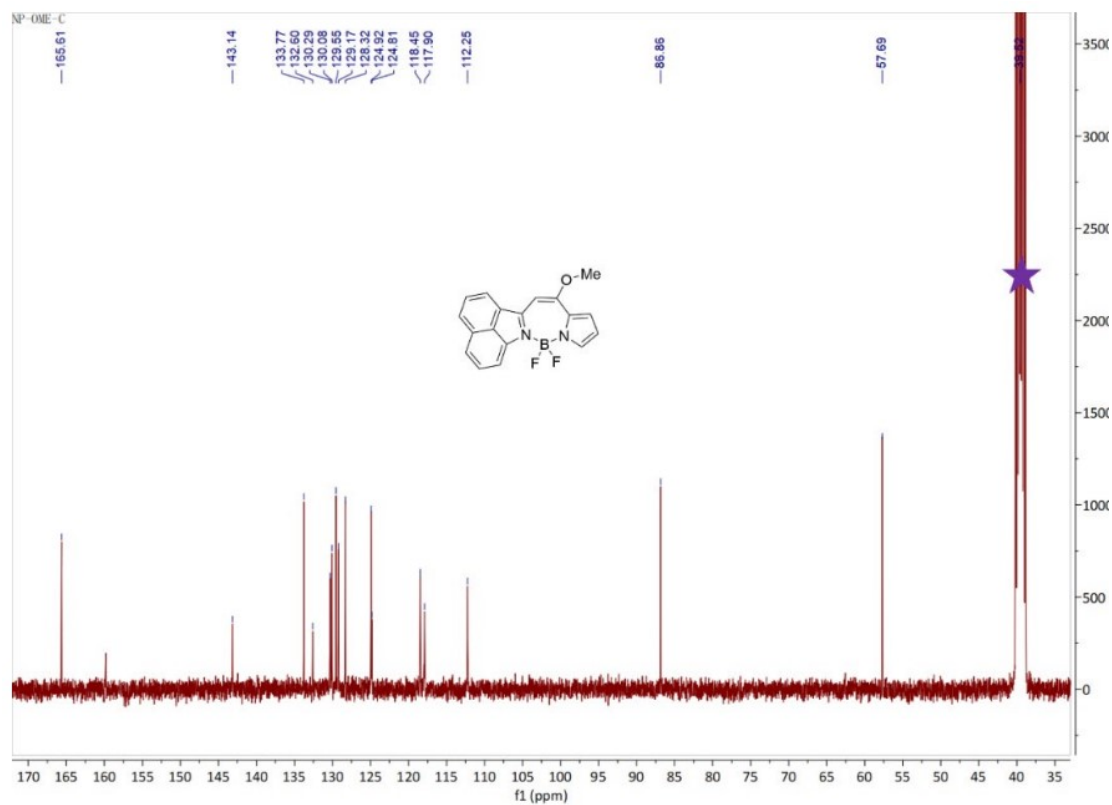


Figure S26 ^{13}C NMR spectra of **10d** in $\text{DMSO}-d_6$ (purple star denotes the solvent residual peak of DMSO at 39.52 ppm as the referenced signal).

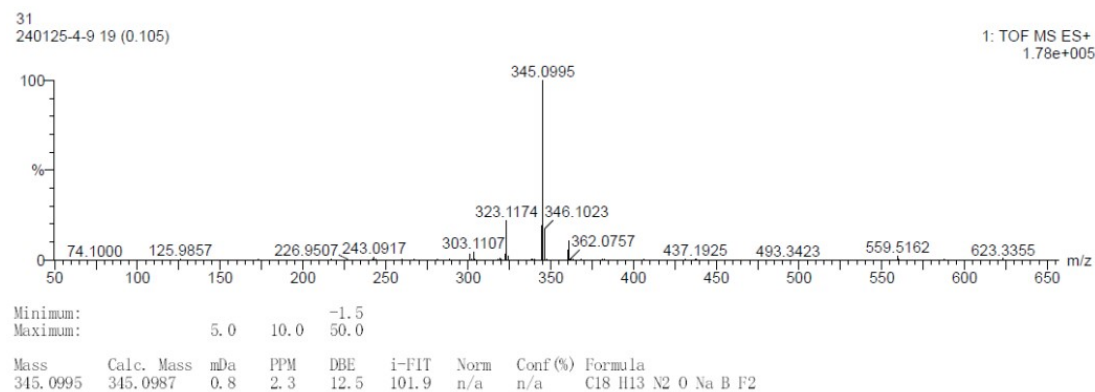


Figure S27 HR-MS spectra of **10d**

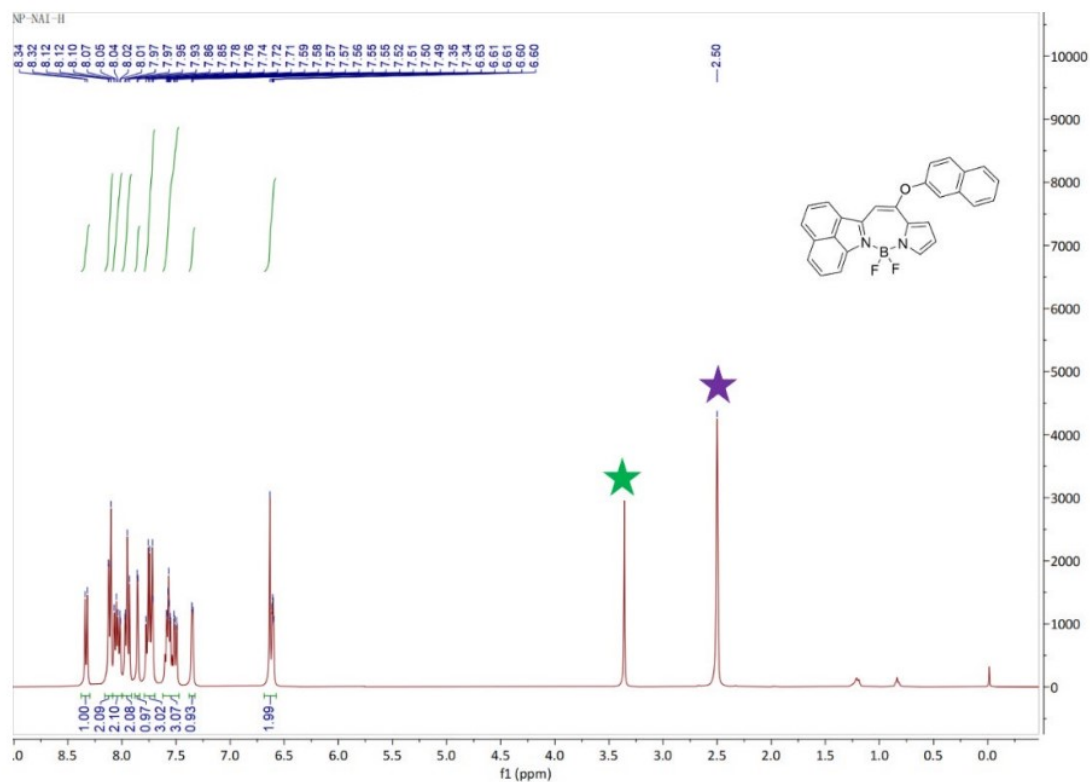


Figure S28 ^1H NMR spectra of **10e** in $\text{DMSO}-d_6$ (green star denotes the residual peak of H_2O , purple star denotes the solvent residual peak of DMSO at 2.50 ppm as the referenced signal).

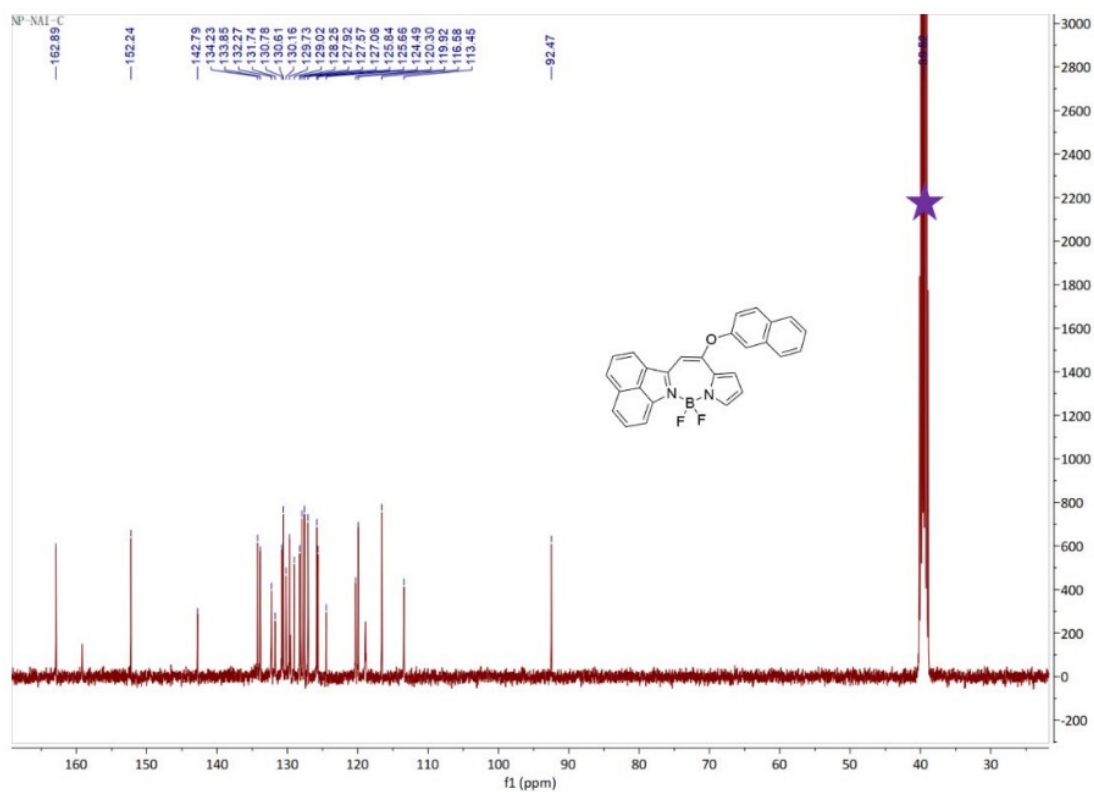


Figure S29 ¹³C NMR spectra of **10e** in DMSO-*d*₆ (purple star denotes the solvent residual peak of DMSO at 39.52 ppm as the referenced signal).

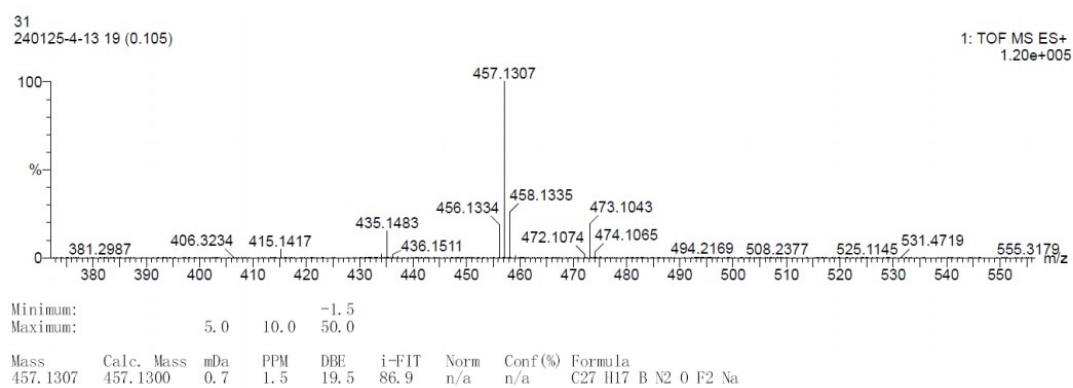


Figure S30 HR-MS spectra of **10e**

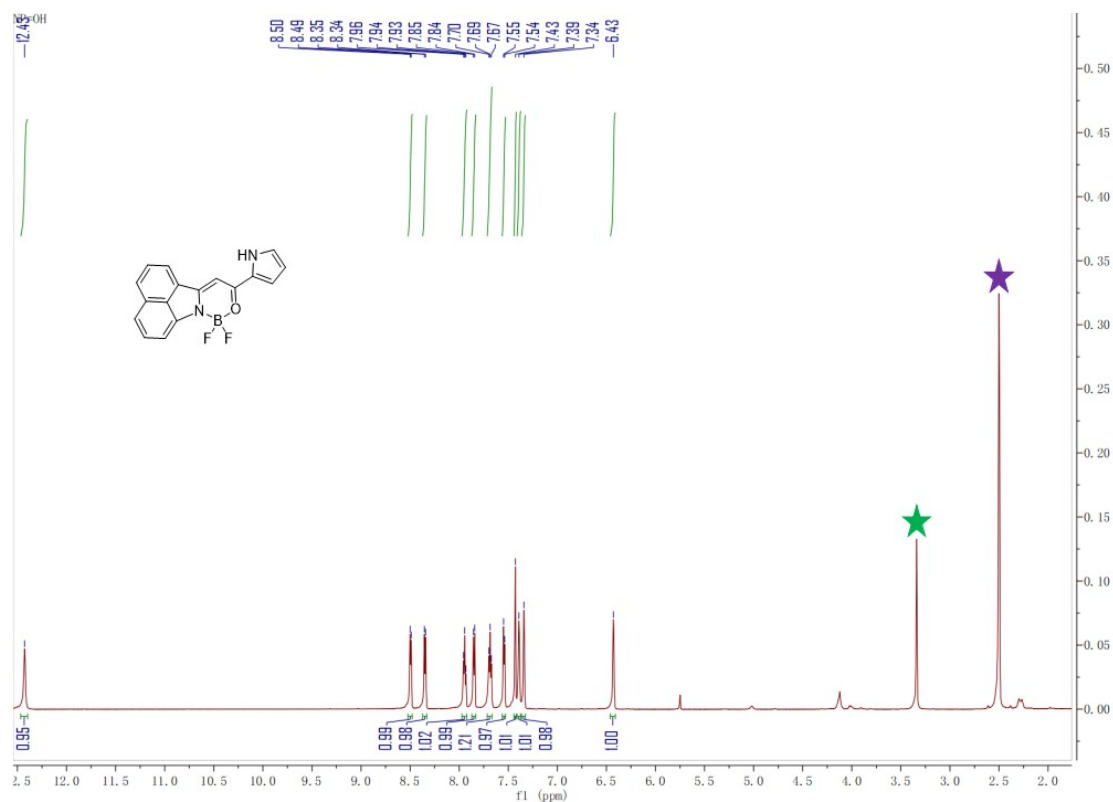


Figure S31 ¹H NMR spectra of **11** in DMSO-d₆ (green star denotes the residual peak of H₂O, purple star denotes the solvent residual peak of DMSO at 2.50 ppm as the referenced signal)

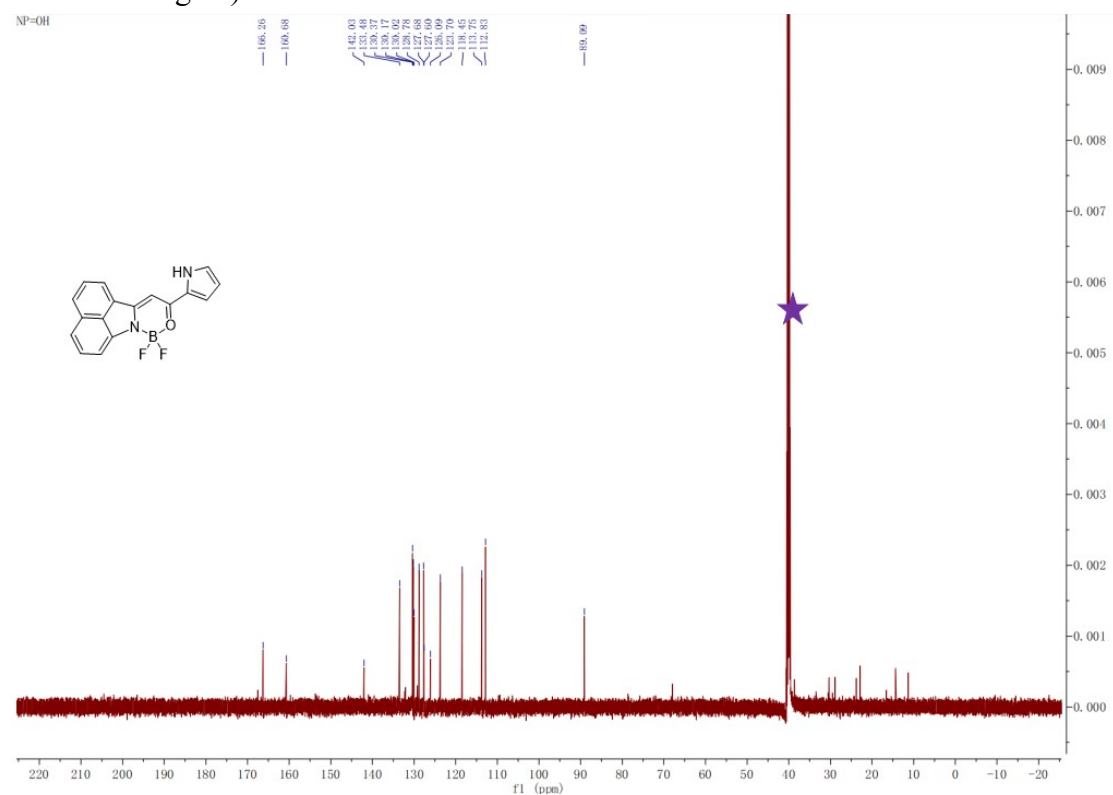


Figure S32 ¹³C NMR spectra of **11** in DMSO-d₆ (purple star denotes the solvent residual peak of DMSO at 40.02 ppm as the referenced signal)

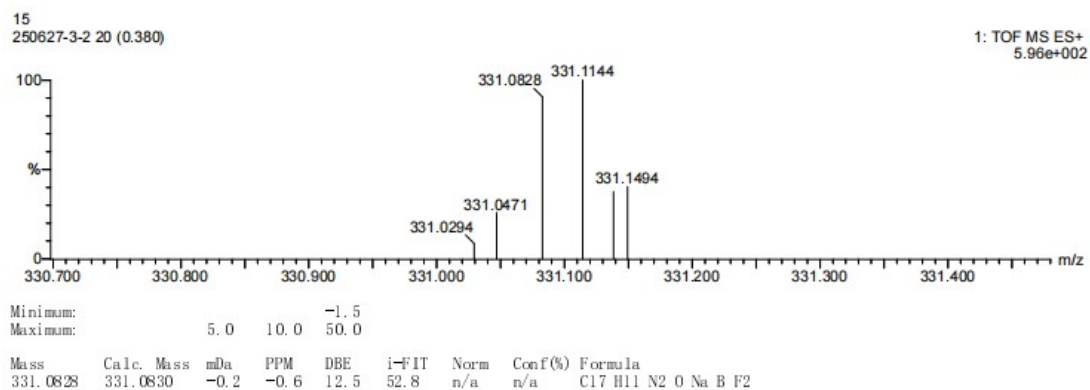


Figure S33 HR-MS spectra of **11**

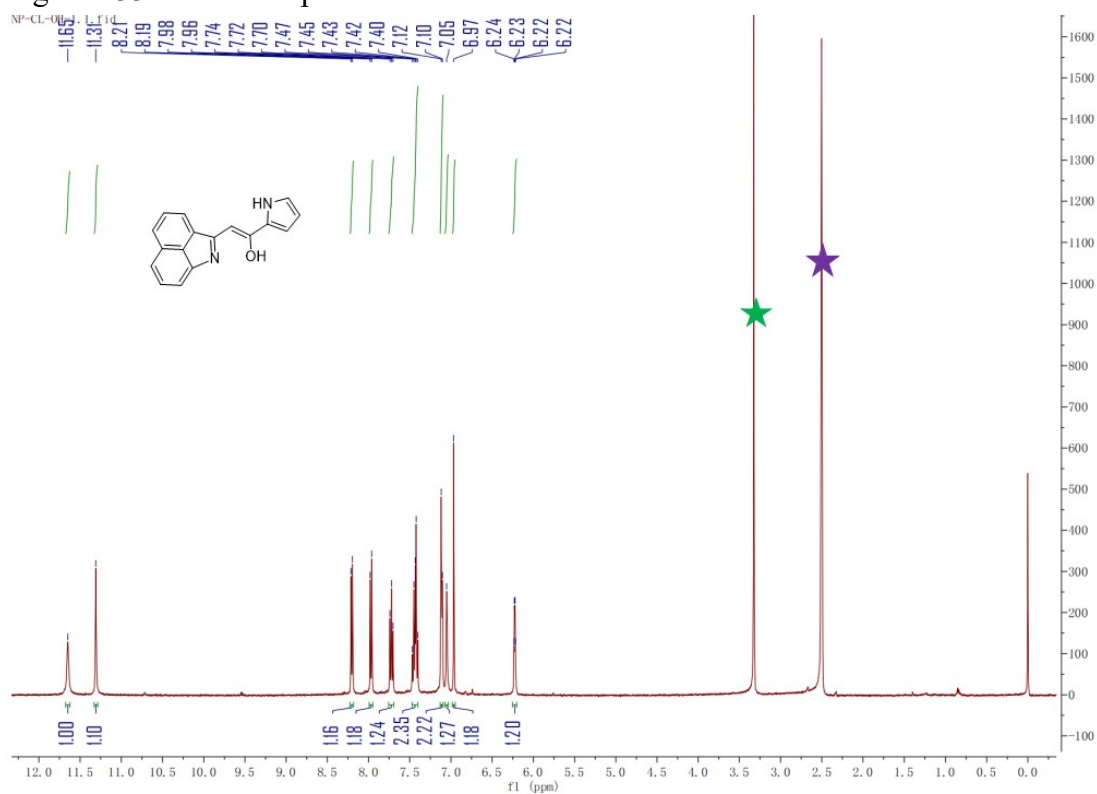


Figure S34 ^1H NMR spectra of **12** in $\text{DMSO}-d_6$ (green star denotes the residual peak of H_2O , purple star denotes the solvent residual peak of DMSO at 2.50 ppm as the referenced signal).

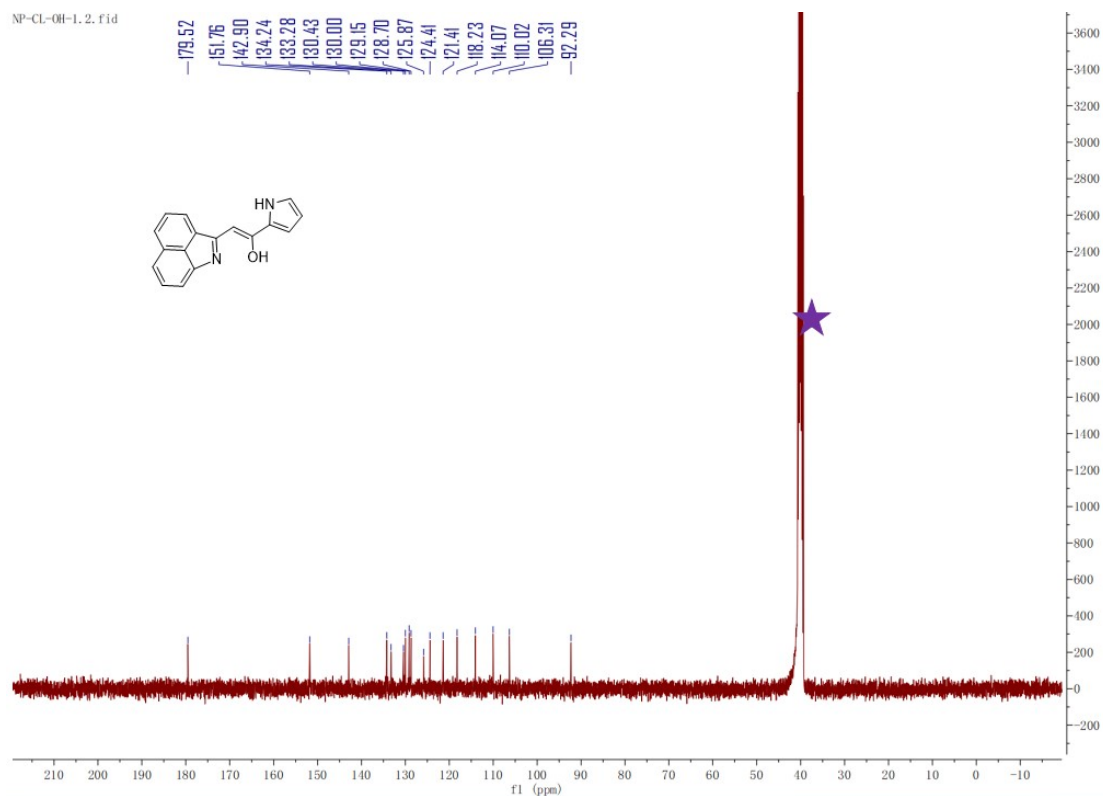


Figure S35 ¹³C NMR spectra of **12** in DMSO-d₆ (purple star denotes the solvent residual peak of DMSO at 40.02 ppm as the referenced signal)

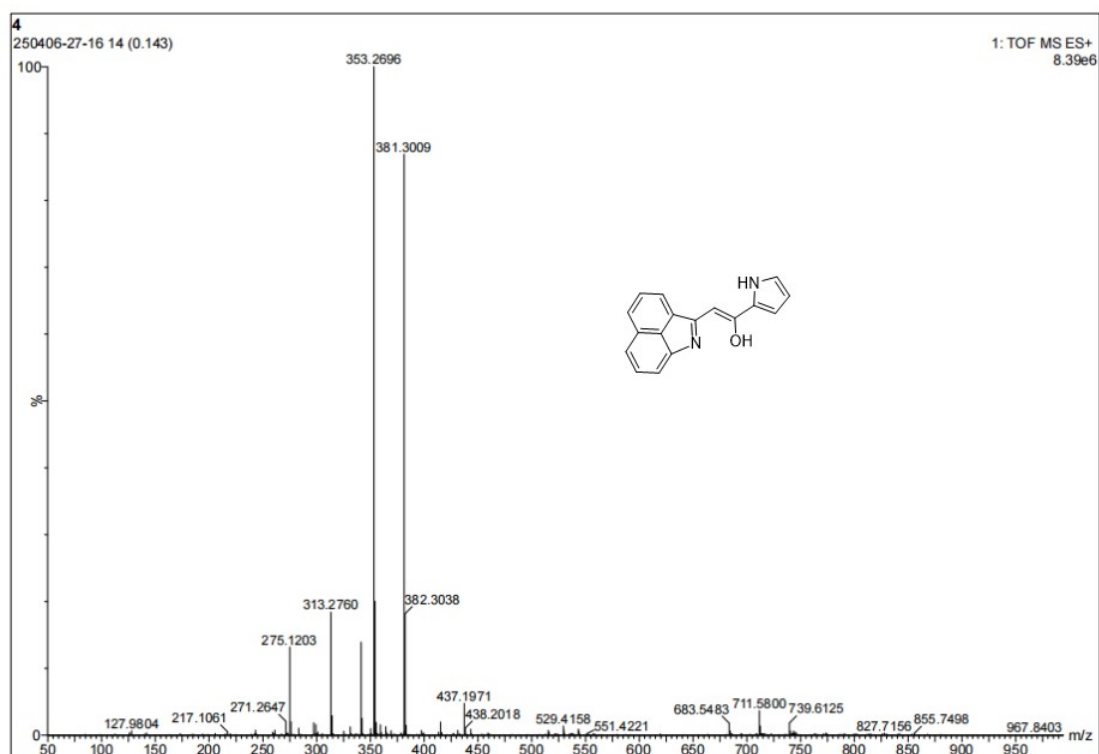


Figure S36 HR-MS spectra of **12**

Table S1 Optimization of the reaction conditions for compound **5**^a.

Entry	Solvent	Catalyst (Loading)	Loading of 1 (equiv)	Yield (%) ^b
1	Toluene	POCl ₃	1.0	12
2	DMSO	POCl ₃	1.0	N.R.
3	DMF	POCl ₃	1.0	N.R.
4	1,4-Dioxane	POCl ₃	1.0	N.R.
5	DCE	POCl ₃	1.0	4
6	Toluene	TiCl ₄	1.0	N.R.
7	Toluene	POCl ₃ (2.0 eq)	1.0	8
8	Toluene	POCl ₃ (3.0 eq)	1.0	19
9	Toluene	POCl ₃ (4.0 eq)	1.0	10
10	Toluene	POCl ₃ (3.0 eq)	1.5	33
11	Toluene	POCl ₃ (3.0 eq)	2.0	28

^a Reaction conditions: All reactions were carried out under reflux conditions with stirring for 3 hours.

^b Isolated yield after purification by column chromatography.

Abbreviations: DMSO, Dimethyl sulfoxide; DMF, N,N-dimethylformamide; DCE, 1,2-Dichloroethane

Table S2 The effect of silica gel on the conversion of **12** to **9**^a.

Entry	Silica gel	Ratio. ^b	Time (h)	Conversion(%)
1	Acidic (300–400)	0.5	2	45
2	Acidic (300–400)	1.0	2	100
3	Acidic (300–400)	2.0	2	100
4	Neutral (300–400)	1.0	2	5
5	--	--	24	trace

^a Reaction conditions: Compound **12** (0.1 mmol) was dissolved in dichloromethane, followed by the addition of silica gel in a certain proportion, and the mixture was stirred at room temperature.

^b The molar ratio of silica gel to compound **12**.

6. UV-Vis and fluorescence data and spectra

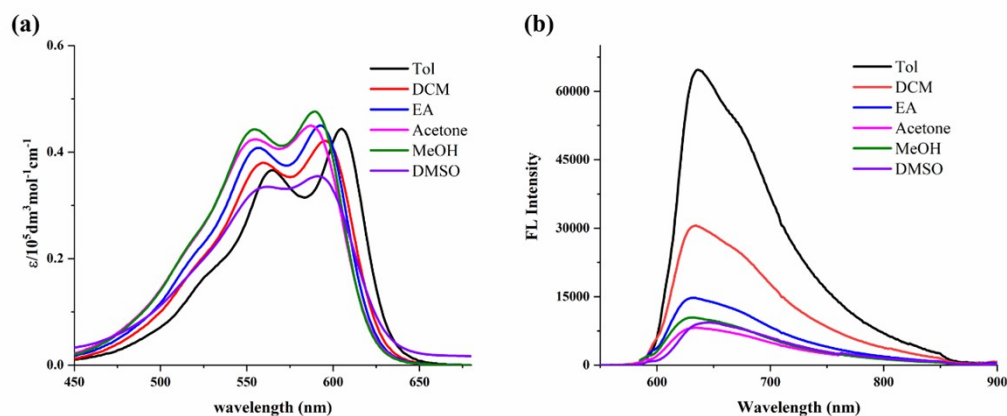


Figure S37 The absorption (a) and emission (b) spectra of **7** in toluene, DCM, EA, Acetone, MeOH, DMSO

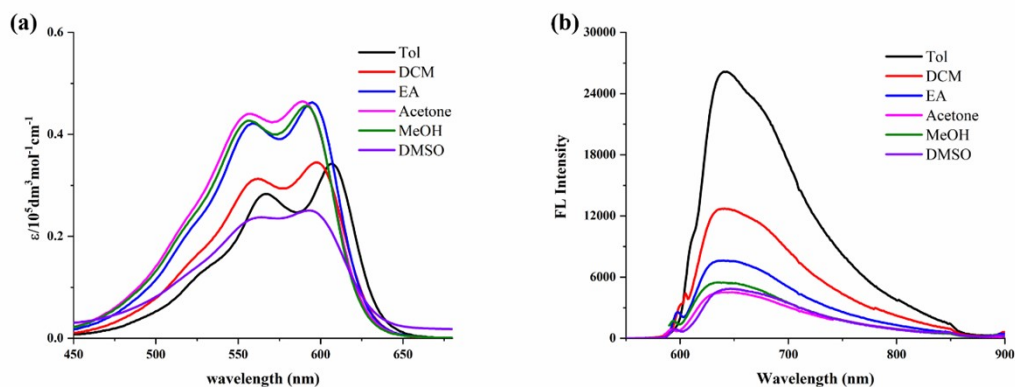


Figure S38 The absorption (a) and emission (b) spectra of **8** in toluene, DCM, EA, Acetone, MeOH, DMSO

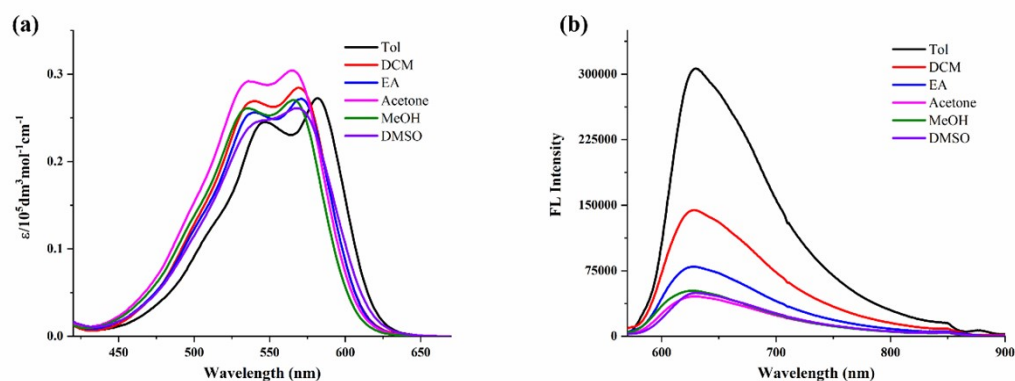


Figure S39 The absorption (a) and emission (b) spectra of **10a** in toluene, DCM, EA, Acetone, MeOH, DMSO

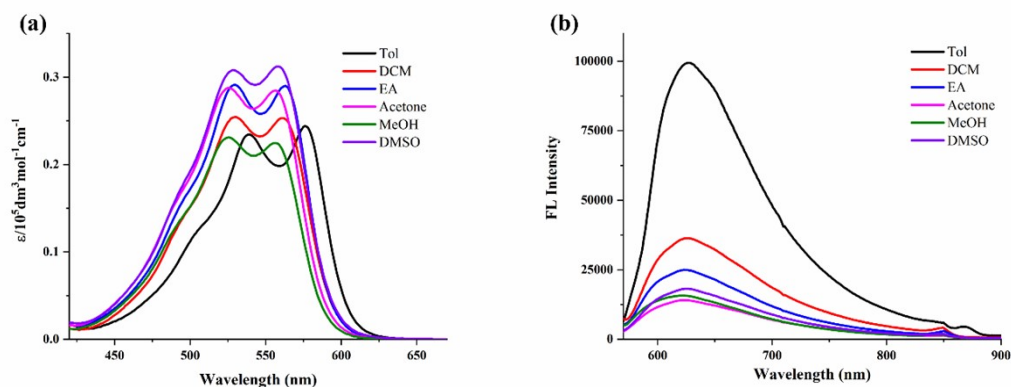


Figure S40 The absorption (a) and emission (b) spectra of **10b** in toluene, DCM, EA, Acetone, MeOH, DMSO

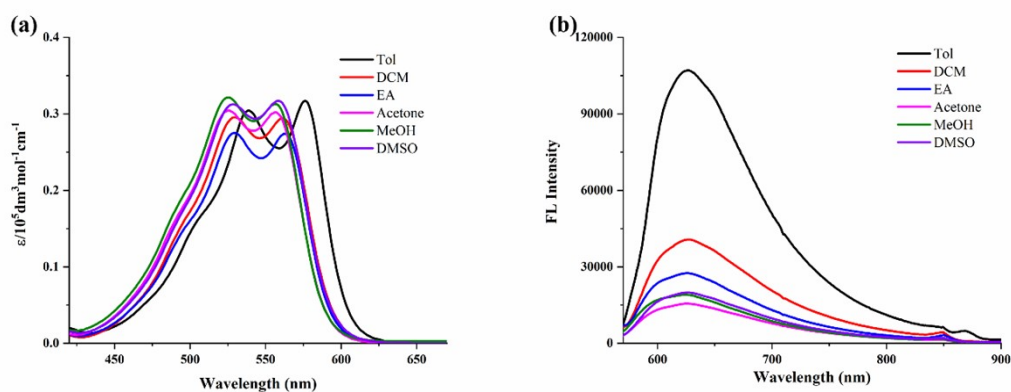


Figure S41 The absorption (a) and emission (b) spectra of **10c** in toluene, DCM, EA, Acetone, MeOH, DMSO

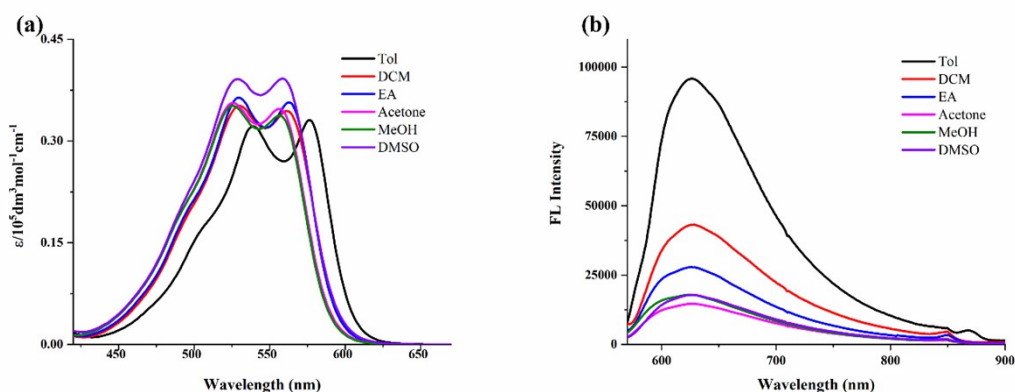


Figure S42 The absorption (a) and emission (b) spectra of **10d** in toluene, DCM, EA, Acetone, MeOH, DMSO

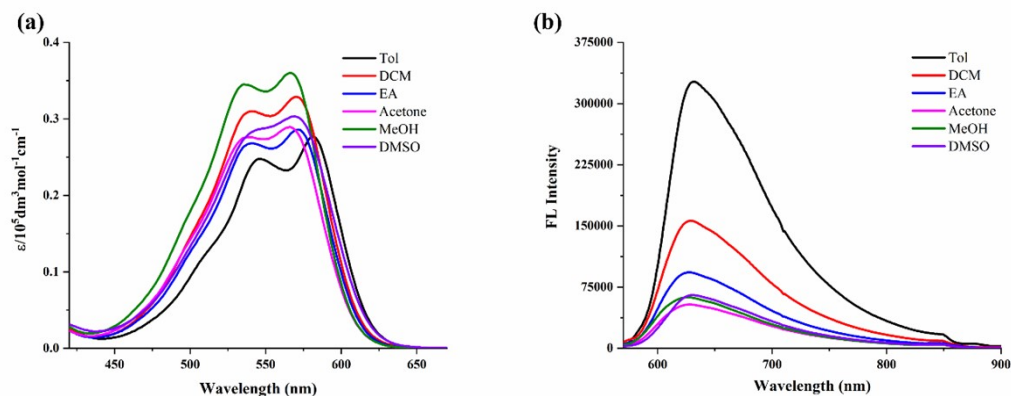


Figure S43 The absorption (a) and emission (b) spectra of **10e** in toluene, DCM, EA, Acetone, MeOH, DMSO

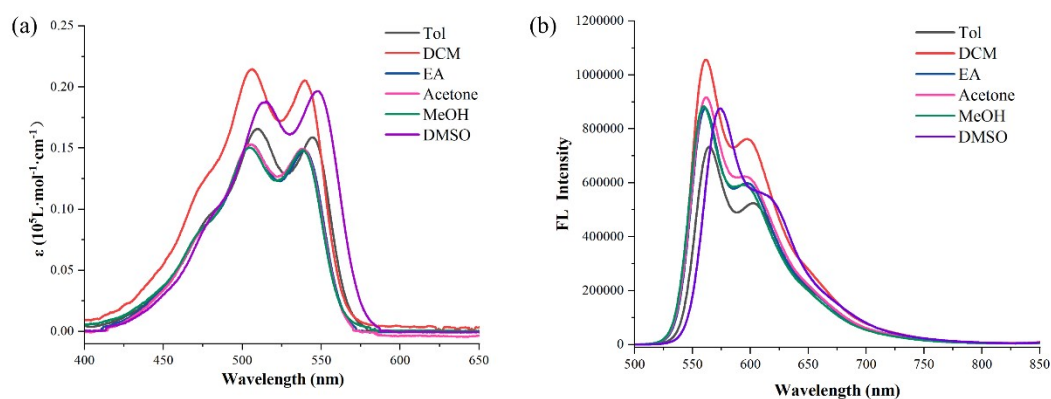


Figure S44 The absorption (a) and emission (b) spectra of **11** in toluene, DCM, EA, Acetone, MeOH, DMSO

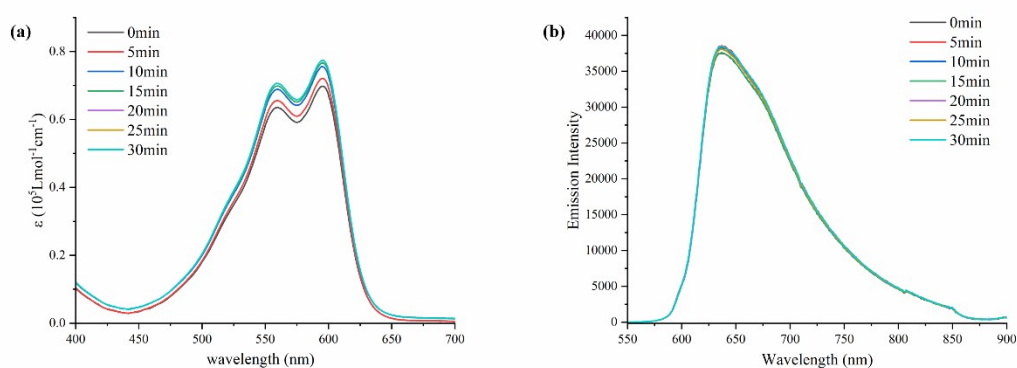


Figure S45 Photostability assessment of compounds **7** under continuous irradiation. (a, b) Evolution of the UV-vis absorption (a) and fluorescence emission (b) spectra of compound **7** under irradiation with a 50 W Xe lamp ($\lambda = 400\text{--}700 \text{ nm}$).

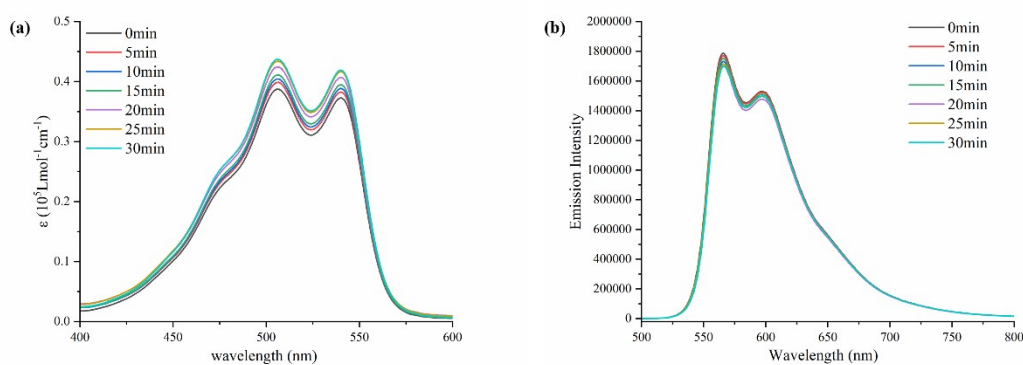


Figure S46 Photostability assessment of compounds **11** under continuous irradiation. (a, b) Evolution of the UV-vis absorption (a) and fluorescence emission (b) spectra of compound **11** under irradiation with a 50 W Xe lamp ($\lambda = 400\text{--}700$ nm).

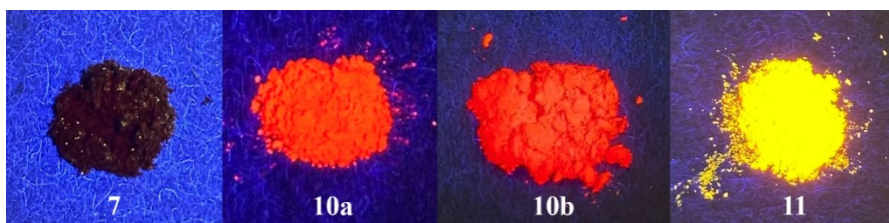


Figure S47 Solid-state fluorescence images for compounds **7**, **10a**, **10b** and **11**.

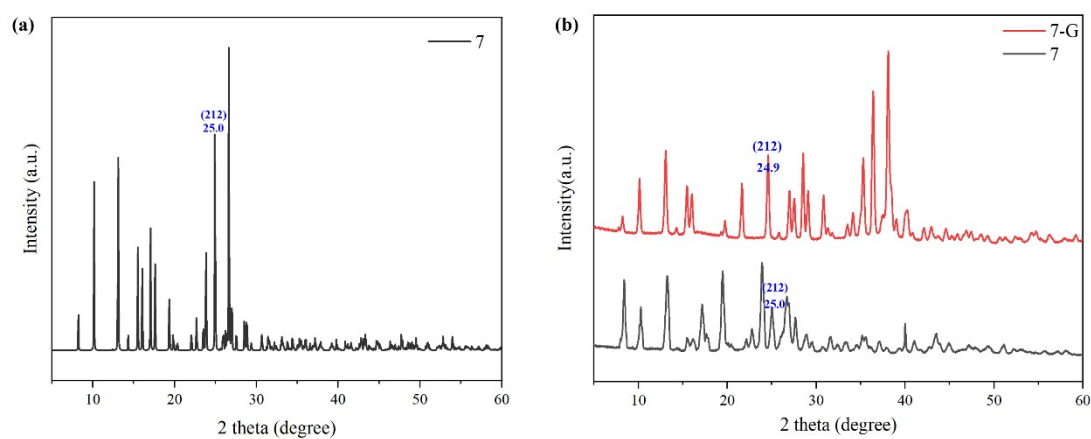


Figure S48 (a) XRD card derived from single-crystal data of **7**. (b) XRD pattern of compound **7** before grinding (**7**, black) and after grinding (**7-G**, red).

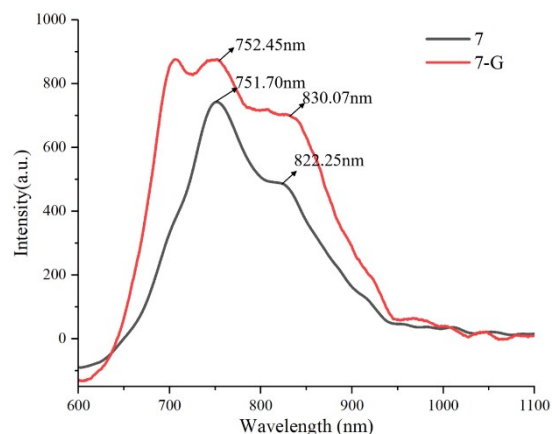


Figure S49 Reflection spectra of powder 7 before grinding (7, black) and after grinding (7-G, red).

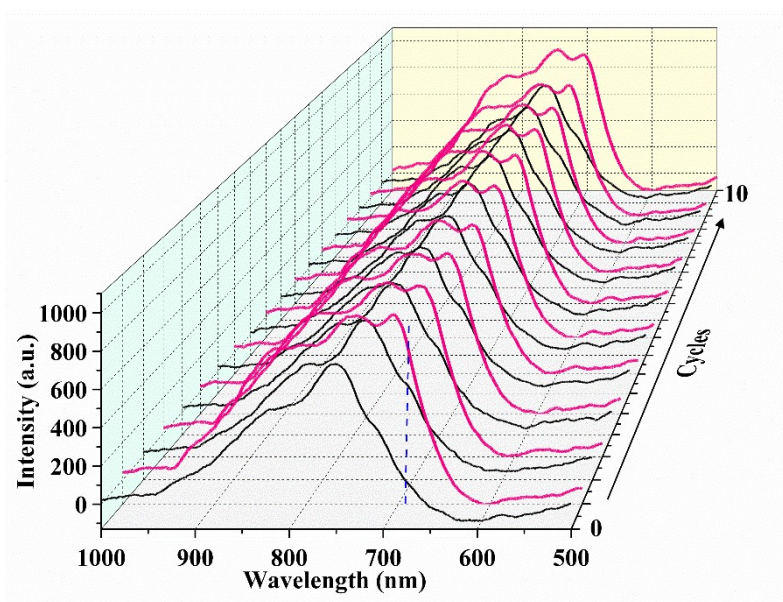


Figure S50 Reflection spectra of powder 7 before (black line) and after grinding (red line), nineteen independent measurements in the initial state, grinding and standing state, respectively. The intensity values at 700.23 nm (marked by the blue line) were extracted to plot the line chart in Figure 1c.

Table S3 Photophysical properties of **BOPYIN**, **BOPYRENPY** in Gonzalez's group, the compound in Gai's group, **7 ~ 8 and 10 ~ 11** in different solvents at room temperature.

Comp.	Solvent	λ_{abs} ($\epsilon/105 \text{ M} \cdot \text{l cm}^{-1}$)(nm)	λ_{ex} (excitation wavelength, nm)	λ_{em} in solvents nm)	Stokes shift		Φ_f^a (%)
					(nm)	(cm^{-1})	
BOPYIN	DCM	470	525	-	55	2228	33
BOPYRENPY in Gonzalez's group	DCM	475	516	-	41	1673	4
The compound in Gai's group	DCM	458	514	-	56	2379	-
7	Toluene	605(0.44) 565(0.37)	605	636	31	806	5
	DCM	595(0.42) 560(0.38)	596	634	38	1033	2
	EA	593(0.45) 558(0.41)	593	632	39	1041	1
	Acetone	587(0.45) 556(0.42)	587	634	47	1263	<1
	MeOH	589(0.48) 555(0.44)	589	632	43	1155	<1
	DMSO	591(0.36) 562(0.34)	591	644	53	1392	<1
8	Toluene	607(0.34) 567(0.28)	607	640	33	849	2
	DCM	598(0.34) 562(0.31)	598	641	43	1122	1
	EA	595(0.46) 559(0.42)	595	636	41	1083	<1
	Acetone	589(0.47) 557(0.44)	589	639	50	1328	<1
	MeOH	591(0.46) 557(0.43)	591	636	45	1197	<1
	DMSO	593(0.25) 564(0.24)	593	646	53	1383	<1
	Toluene	582(0.28)	582	630	48	1300	5

		547(0.25)					
	DCM	569(0.29) 541(0.27)	569	628	59	1651	2
	EA	571(0.27) 540(0.26)	571	629	58	1615	1
	Acetone	565(0.31) 536(0.29)	565	628	63	1776	<1
	MeOH	566(0.27) 535(0.26)	566	627	61	1719	<1
	DMSO	568(0.26)	568	630	62	1733	<1
10b	Toluene	576(0.25) 539(0.24)	576	627	51	1412	1
	DCM	561(0.25) 530(0.25)	561	627	66	1876	<1
	EA	563(0.29) 530(0.29)	563	623	60	1774	<1
	Acetone	556(0.28) 526(0.28)	556	623	67	1934	<1
	MeOH	556(0.22) 526(0.23)	556	623	67	1934	<1
	DMSO	558(0.31) 529(0.31)	558	626	68	1947	<1
10c	Toluene	576(0.32) 539(0.31)	576	627	51	1412	2
	DCM	561(0.28) 530(0.28)	561	626	65	1851	<1
	EA	563(0.27) 530(0.27)	563	626	63	1788	<1
	Acetone	556(0.35) 526(0.36)	556	626	70	2011	<1
	MeOH	556(0.31) 526(0.32)	556	624	68	1960	<1
	DMSO	558(0.32) 529(0.32)	558	626	68	1947	<1
10d	Toluene	576(0.33) 539(0.32)	576	627	51	1412	2
	DCM	561(0.35) 530(0.35)	561	629	68	1927	<1
	EA	563(0.36) 530(0.36)	563	626	63	1788	<1
	Acetone	556(0.35) 526(0.36)	556	626	70	2011	<1
	MeOH	556(0.33)	556	625	69	1986	<1

		526(0.35)					
	DMSO	558(0.39) 529(0.39)	558	627	69	1972	<1
10e	Toluene	581(0.27) 546(0.25)	581	632	51	1389	4
	DCM	570(0.33) 541(0.31)	570	629	59	1646	2
	EA	571(0.28) 540(0.27)	571	628	57	1590	1
	Acetone	566(0.29) 539(0.27)	566	629	63	1770	<1
	MeOH	566(0.36) 535 0.35)	566	626	60	1693	<1
	DMSO	569(0.30)	569	631	62	1727	<1
11	Toluene	544(0.16) 509(0.17)	544	603 565	59	1799	88
	DCM	539(0.21) 506(0.22)	539	597 562	58	1803	86
	EA	539(0.15) 506(0.15)	539	597 561	58	1803	68
	Acetone	537(0.15) 505(0.15)	537	562	25	828	67
	MeOH	538(0.15) 504(0.15)	538	594 560	56	1752	56
	DMSO	547(0.20) 515(0.19)	547	574	27	860	99

7. Single Crystal

Table S4 Crystal data for **7**, **9**, **10a**, and **11**

Identification code	7	9	10a	11
Empirical formula	C ₁₇ H ₁₀ BF ₂ N ₂ Cl	C ₁₇ H ₁₂ N ₂ O	C ₂₃ H ₁₅ BN ₂ O F ₂	C ₁₇ H ₁₁ BF ₂ N ₂ O
Formula weight	349.14	260.29	407.11	308.09
Temperature/K	297.7(2)	100.01(11)	99.99(10)	170.00(10)
Crystal system	monoclinic	orthorhombic	triclinic	monoclinic
Space group	P2 ₁ /c	Pbca	P-1	P2 ₁ /c
a/Å	8.72703(19)	5.1777(2)	10.1116(2)	9.6144(2)
b/Å	7.57330(14)	19.0358(12)	11.6324(2)	8.74800(10)
c/Å	21.4926(4)	24.8301(14)	30.3083(5)	16.3991(3)
α/°	90	90	94.5670(10)	90
β/°	90.3969(19)	90	97.121(2)	105.208(2)

$\gamma/^{\circ}$	90	90	90.226(2)	90
Volume/ \AA^3	1420.46(5)	2447.3(2)	3525.85(11)	1330.97(4)
Z	4	8	8	4
$\rho_{\text{calc}}/\text{g/cm}^3$	1.527	1.413	1.447	1.537
μ/mm^{-1}	2.579	0.715	0.854	0.969
F(000)	664	1088	1584	632
Crystal size/ mm^3	$0.14 \times 0.12 \times 0.11$	$0.13 \times 0.11 \times 0.09$	$0.15 \times 0.12 \times 0.1$	$0.14 \times 0.13 \times 0.12$
Radiation	Cu K_{α} ($\lambda = 1.54184$)	Cu K_{α} ($\lambda = 1.54184$)	Cu K_{α} ($\lambda = 1.54184$)	Cu K_{α} ($\lambda = 1.54184$)
2 θ range for data collection/ $^{\circ}$	8.22 to 133.2	9.292 to 145.738	5.9 to 146.82	9.532 to 145.642
Index ranges	$-10 \leq h \leq 10$, $-9 \leq k \leq 4$, $-25 \leq l \leq 25$	$-4 \leq h \leq 6$, $-23 \leq k \leq 22$, $-29 \leq l \leq 30$	$-12 \leq h \leq 12$, $-10 \leq k \leq 14$, $-37 \leq l \leq 37$	$-11 \leq h \leq 11$, $-10 \leq k \leq 8$, $-18 \leq l \leq 20$
Reflections collected	6237	16744	48774	8972
Independent reflections	2495 [$R_{\text{int}} = 0.0233$, $R_{\text{sigma}} = 0.0230$]	2344 [$R_{\text{int}} = 0.1212$, $R_{\text{sigma}} = 0.0541$]	13651 [$R_{\text{int}} = 0.0657$, $R_{\text{sigma}} = 0.0576$]	2572 [$R_{\text{int}} = 0.0168$, $R_{\text{sigma}} = 0.0156$]
Data/restraints/parameters	2495/0/209	2344/0/181	13651/0/1045	2572/0/209
Goodness-of-fit on F^2	1.081	1.319	1.15	1.037
Final R indexes [$I \geq 2\sigma(I)$]	$R_1 = 0.0345$, $wR_2 = 0.0945$	$R_1 = 0.1024$, $wR_2 = 0.2277$	$R_1 = 0.0797$, $wR_2 = 0.2608$	$R_1 = 0.0309$, $wR_2 = 0.0815$
Final R indexes [all data]	$R_1 = 0.0368$, $wR_2 = 0.0961$	$R_1 = 0.1114$, $wR_2 = 0.2328$	$R_1 = 0.0917$, $wR_2 = 0.2691$	$R_1 = 0.0334$, $wR_2 = 0.0834$
Largest diff. peak/hole / $e \text{\AA}^{-3}$	0.23/-0.19	0.33/-0.28	0.50/-0.51	0.25/-0.16
CCDC	2498678	2498676	2498680	2498677

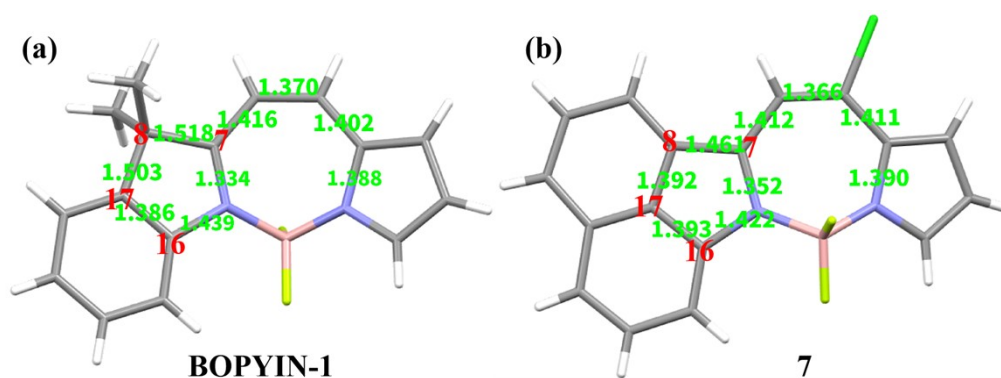


Figure S51 The typical bond lengths of **BOPYIN-1**² and compound **7**

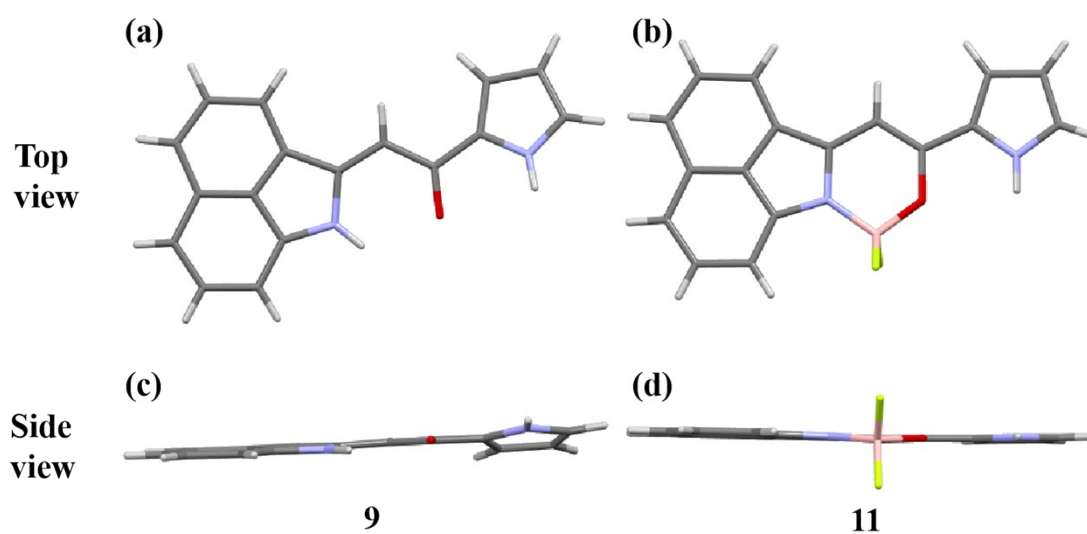


Figure S52 Single-crystal structures of **9** and **11** (yellow for the F atom, purple for the N atom, gray for the C atom, pink for the B atom, red for O atom, while for H atom).

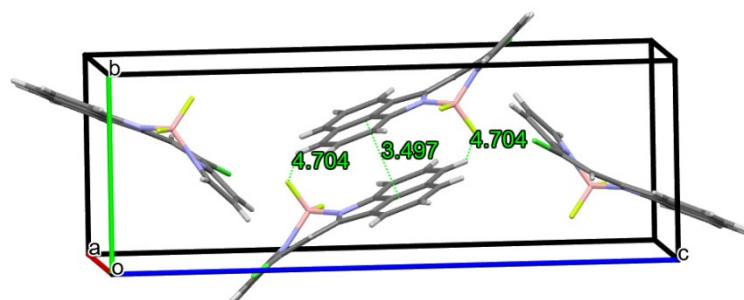


Figure S53 The packing structure of compound **7**

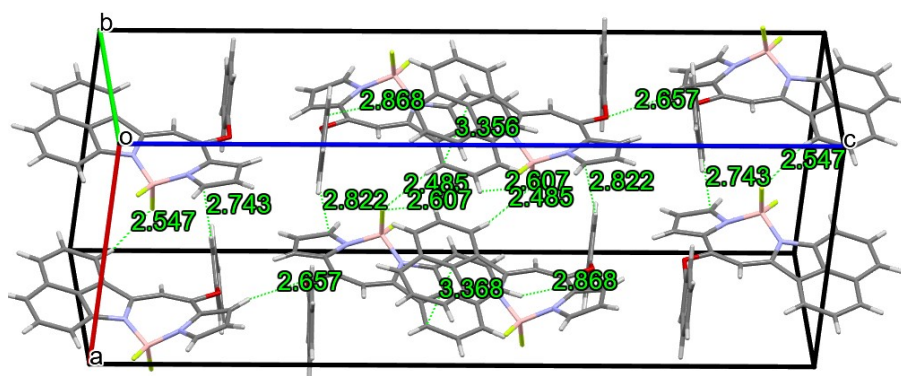


Figure S54 The packing structure of compound **10a**

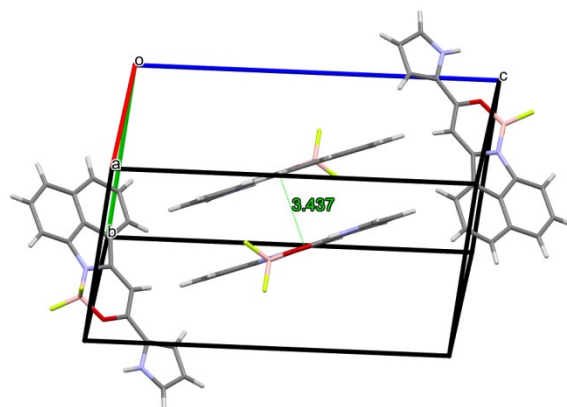


Figure S55 The packing structure of compound **11**

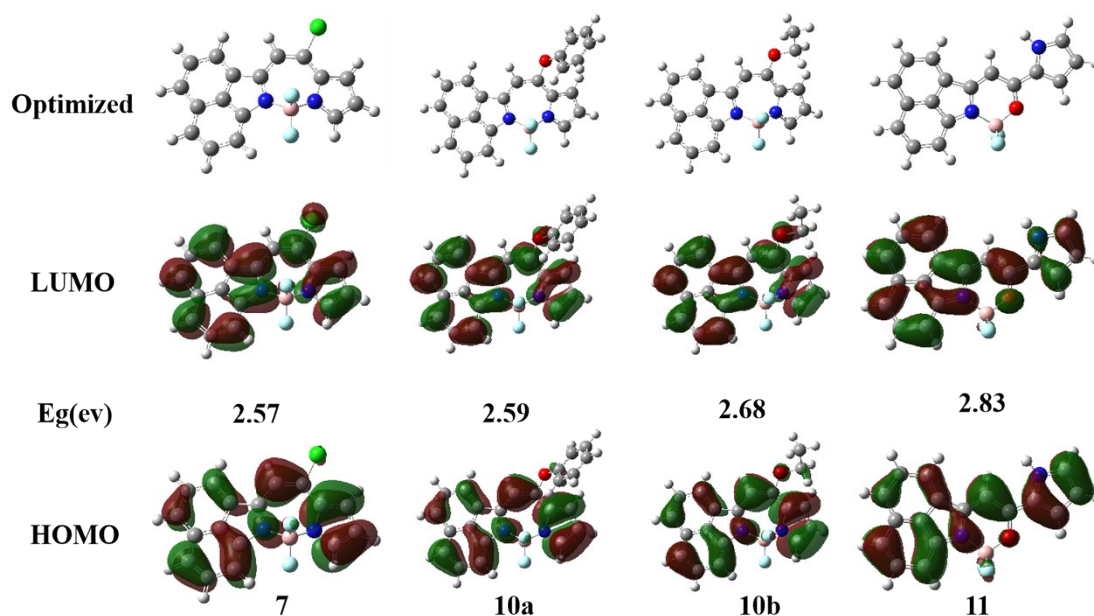


Figure S56 Visualization of HOMO (H) and LUMO (L) with associated energy gaps (Eg/eV) for compounds **7**, **10a**, **10b** and **11**. (B3LYP/6-311G(d,p) level)

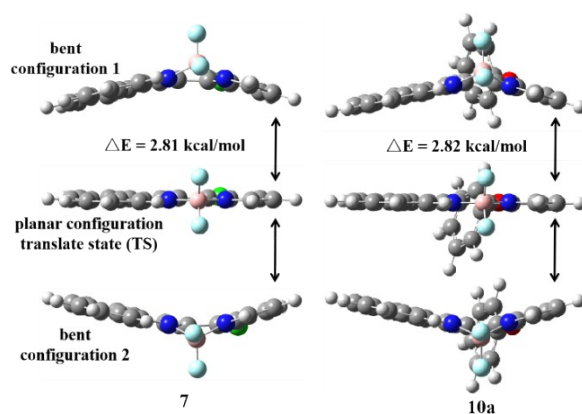


Figure S57 The bent, planar configurations (TS) and activity energies (ΔE) of compound **7** and **10a**.

Table S5 Selected energies in S_1 , T_n and the energy gaps for compounds **7** and **10a**

compound	State	Energy (eV)	S_1-T_2 (eV)
7	T_1	1.2465	0.0636
	T_2	2.4216	
	S_1	2.4852	
10a	T_1	1.4984	0.0662
	T_2	2.5648	
	S_1	2.6310	

References

1. M. J. Frisch, G. W. Trucks, H. B. Schlegel, G. E. Scuseria, M. A. Robb, J. R. Cheeseman, G. Scalmani, V. Barone, G. A. Petersson, H. Nakatsuji, X. Li, M. Caricato, A. V. Marenich, J. Bloino, B. G. Janesko, R. Gomperts, B. Mennucci, H. P. Hratchian, J. V. Ortiz, A. F. Izmaylov, J. L. Sonnenberg, Williams, F. Ding, F. Lipparini, F. Egidi, J. Goings, B. Peng, A. Petrone, T. Henderson, D. Ranasinghe, V. G. Zakrzewski, J. Gao, N. Rega, G. Zheng, W. Liang, M. Hada, M. Ehara, K. Toyota, R. Fukuda, J. Hasegawa, M. Ishida, T. Nakajima, Y. Honda, O. Kitao, H. Nakai, T. Vreven, K. Throssell, Jr. J. A. Montgomery, J. E. Peralta, F. Ogliaro, M. J. Bearpark, J. J. Heyd, E. N. Brothers, K. N. Kudin, V. N. Staroverov, T. A. Keith, R. Kobayashi, J. Normand, K. Raghavachari, A. P. Rendell, J. C. Burant, S. S. Iyengar, J. Tomasi, M. Cossi, J. M. Millam, M. Klene, C. Adamo, R. Cammi, J. W. Ochterski, R. L. Martin, K. Morokuma, O. Farkas, J. B. Foresman, D. J. Fox, Gaussian 16, Revision C. 01, Gaussian, Inc., Wallingford CT, 2016.